# Phase separation and fluid mixing in subseafloor back arc hydrothermal systems: A microthermometric and oxygen isotope study of fluid inclusions in the barite-sulfide chimneys of the Lau basin

Christophe Lécuyer, Michel Dubois, Christian Marignac, G•rard Gruau, Yves Fouquet, Claire Ramboz

JOURNAL OF GEOPHYSICAL RESEARCH, VOL. 104, NO. B8, PAGES 17,911–17,927, AUGUST 10, 1999

# Phase separation and fluid mixing in subseafloor back arc hydrothermal systems: A microthermometric and oxygen isotope study of fluid inclusions in the barite-sulfide chimneys of the Lau basin

Christophe Lécuyer,[1] Michel Dubois,[2] Christian Marignac,[3] Gérard Gruau,[4] Yves Fouquet,[5] and Claire Ramboz[6]

**Abstract.** Fluid inclusions in barite and sulfide in chimneys (both active and inactive) from three hydrothermal sites of the back arc Lau basin were studied with microthermometric and isotopic methods to determine the chemistry and evolution of hydrothermal aqueous fluids. Strontium isotope compositions of sulfides from the Lau basin reflect the presence of anhydrite and barite inclusions. The $^{87}Sr/^{86}Sr$ ratios of these two sulfate minerals vary from 0.7045 to 0.7078 and are interpreted as the result of mixing between various proportions of the hydrothermal end-member and pure seawater. The microthermometric study of fluid inclusions reveals that mixing with seawater involved different kinds of aqueous fluid end-members. A high-temperature Mg-depleted end-member of high salinity (≥5.5 wt % eq NaCl) was found at the Vai Lili site. A uncommon low-temperature Mg-rich end-member was also identified at the Hine Hina site in association with barite deposition. At the Vai Lili site, very low salinity fluids were produced in addition to a very saline brine (≥30 wt % NaCl) that was trapped inside anhydrite precipitated from an active vent at a temperature of 342°C. Oxygen isotope ratios of water inclusions range from 2‰ to 4.4‰ for chalcopyrite, barite, and sphalerite minerals. The $^{18}O$ enrichment and the high salinities of many fluids from the Lau basin are accounted for by the specificity of the back arc setting. This non mid-ocean ridge setting is characterized by the shallow depth of the hydrothermal systems that allows frequent unmixing of high-temperature liquids. The abundance of silicic magmas also provided magmatic fluids (including brines) that mixed with seawater-derived aqueous fluids.

## 1. Introduction

Back arc environments are thought to correspond closely to that of ancient major sulfide deposits on land where massive sulfides are commonly associated with felsic volcanic rocks [*Franklin et al.*, 1981; *Scott*, 1985, 1987; *Rona*, 1988; *Halbach et al.*, 1989]. These onshore deposits are currently believed to have formed in island-arc settings or marginal basins [*Franklin et al.*, 1981; *Cathles et al.*, 1983; *Scott*, 1985, 1987; *Sawkins*, 1990]. The fundamental ore-forming processes in these environments are similar to those described at seafloor spreading centers [*Halbach et al.*, 1989; *Herzig et al.*, 1990; *Fouquet et al.*, 1993]. However, the mineralogy and chemistry of the resulting deposits are largely controlled by source-rock lithology reflective of the tectonic setting [*Fouquet et al.*, 1993].

The Lau basin is a good example of a back arc system environment. High-temperature hydrothermal fields were discovered and sampled by submersible in the Valu Fa Ridge of the Lau back-arc basin during the *Nautilau* cruise in 1989 [*Fouquet et al.*, 1991a]. These deposits are well-studied, from the point of view of their mineralogical content [*Fouquet et al.*, 1993], their isotopic composition [*Fouquet and Marcoux*, 1995] and the nature of present-day venting fluids [*Fouquet et al.*, 1991b; 1993]. In addition, gold occurrence was described [*Herzig et al.*, 1993].

These deposits offer a good opportunity to address several questions relative to the origin of hydrothermal fluids and the processes operating in the oceanic crust (in particular, fluid mixing and phase separation) of back arc ridges. This will be achieved in this work through the combined determination of the thermal, chemical, and isotopic evolution of the hydrothermal fluids that have deposited the sulfide and sulfate minerals from the three main hydrothermal fields of the Valu Fa Ridge. The combination of strontium isotope measurements of sulfide and sulfate minerals and the microthermometric and oxygen isotope analyses of their fluid inclusions will be used to identify the processes of chemical exchange between solid and fluid phases, fluid phase separation, and fluid mixing in the oceanic crust.

[1]Laboratoire de Sciences de la Terre, CNRS UMR 8515, Ecole Normale Supérieure de Lyon, France.
[2]Sciences de la Terre, Université des Sciences et Technologies de Lille, Villeneuve d'Ascq, France.
[3]Ecole des Mines de Nancy, Nancy and CRPG-CNRS, Vandoeuvre-lès-Nancy, France.
[4]Géosciences Rennes, CNRS UPR 4661, Université de Rennes I, Campus de Beaulieu, Rennes, France.
[5]IFREMER, Centre de Brest, Plouzane, France.
[6]CRSCM-CNRS, Orléans, France.



Paper number 1999JB900121.
0148-0227/99/1999JB900121$09.00

## 2. Geological Setting

### 2.1. Lau Basin and Valu Fa Ridge

The Valu Fa Ridge is the active back arc spreading center of the southern Lau basin between 19°20' and 22°50'S [*Morton and Sleep*, 1985; *von Stackelberg et al.*, 1988; *Foucher et al.*, 1988; *Parson et al.*, 1990; *Morton and Pohl*, 1990]. Opening started 1 Myr ago with 3 cm/yr half-spreading rate. The Valu Fa Ridge, located only 20 to 40 km west of the active Tofua volcanic arc (Figure 1) is more than 150 km long and generally strikes 20° (NNE); it is 2-5 km wide and rises 500-600 m above the surrounding seafloor. Small non transform offsets and an overlapping spreading center (OSC) divide the ridge into three major segments: the southern, central, and northern Valu Fa Ridge [*von Stackelberg et al.*, 1988; *von Stackelberg and von Rad*, 1990] which are arranged en echelon a few kilometers apart. The Southern Valu Fa Ridge is still propagating southward. The individual volcanic segments consist of small, straight ridges, predominantly with steep slopes. The high gas content of the magma has produced highly vesicular and brecciated lavas, while major faults and fissures are less numerous than at mid-oceanic ridges. Compared to mid-oceanic ridges, volcanic rocks of the Lau basin are more differentiated, comprising Fe-Ti basalts and andesites, with lesser dacites and rhyolites [*Hawkins and Melchior*, 1985; *Jenner et al.*, 1987; *Volpe et al.*, 1988; *Boespflug et al.*, 1990; *Frenzel et al.*, 1990; *Loock et al.*, 1990; *Sunkel*, 1990]. At the central Valu Fa Ridge, a 1 to 2.5 km wide magma chamber has been imaged seismically under the neovolcanic zone at a depth of about 3 km below the seafloor [*Morton and Sleep*, 1985; *Collier and Sinha*, 1990]. The magma chamber was imaged beneath an entire 35 km long segment including the OSC and the Vai Lili active hydrothermal field. Using the dissolved silica concentrations in the Vai Lili fluids, *Fouquet et al.* [1993] estimated the depth of the high temperature reaction zone (HTRZ) beneath the vents at about 1 km below the seafloor, 2 km above the top of the seismically imaged magma chamber.

### 2.2. Major Hydrothermal Fields and Their Sulfide Deposits [*Fouquet et al.*, 1993 and references therein]

Three main hydrothermal fields were recognized: Hine Hina, Vai Lili, and White Church (Figure 1). According to the findings of *Fouquet et al.* [1993], they correspond to three different volcanic and tectonic stages (Figure 2). The type of

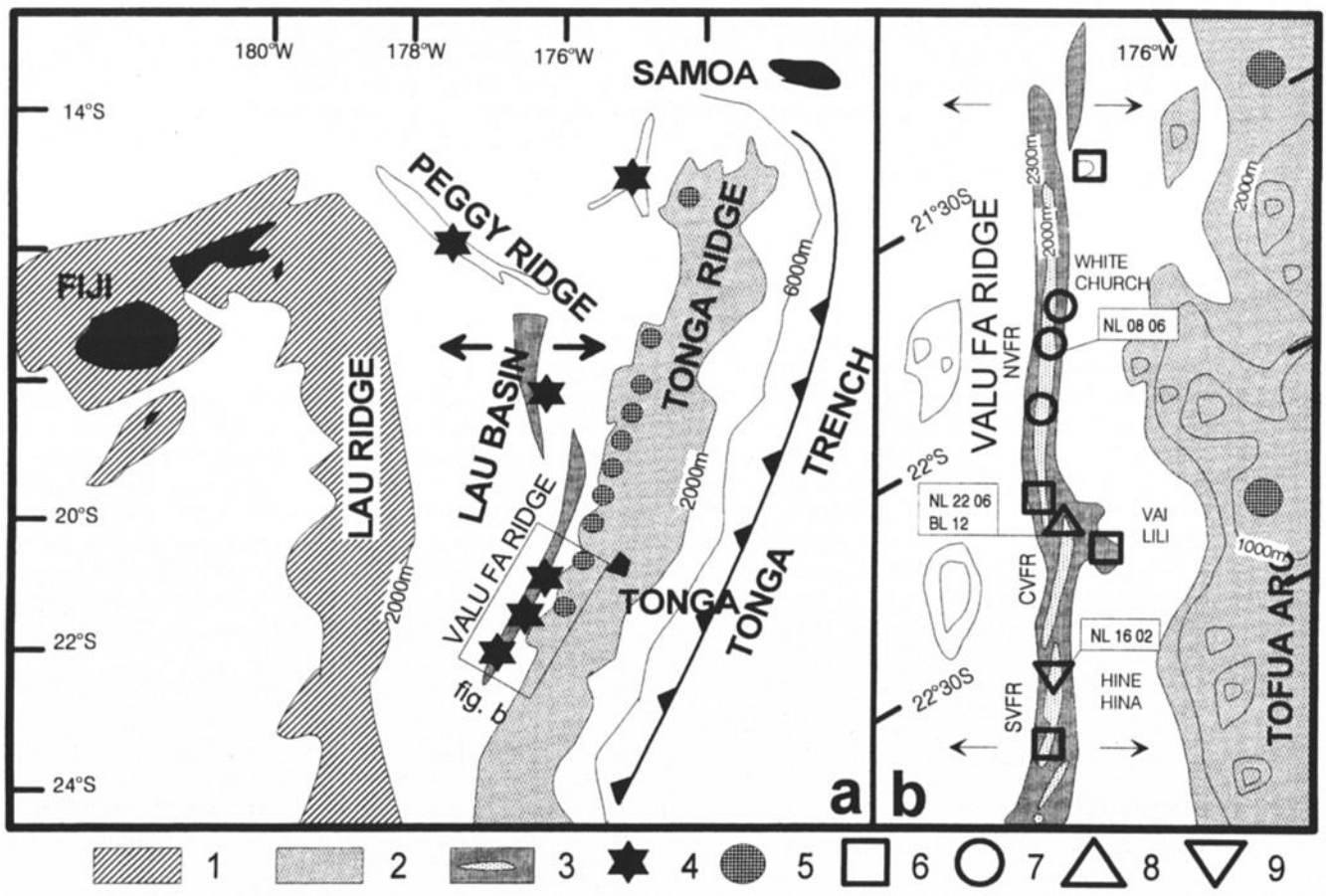


**Figure 1.** (a) General map of the Lau back arc basin. (b) Location of the hydrothermal fields along the Valu Fa Ridge near the active Tofua island arc. The four diving areas (1,2,3,4) are shown together with the names of the three main hydrothermal fields (Hine Hina, Vai Lili and White Church). Nine hydrothermal occurrences were found along the Valu Fa Ridge: 1, Lau Ridge (remnant island arc); 2, Tonga Ridge (island arc); 3, active back arc spreading, (light dots are above 2000 m); 4, hydrothermal occurrences in the Lau basin; 5, active volcanoes (active part of the island arc (Tofua arc)); 5, Fe-Mn deposits; 7, Ba-Zn deposits; 8, Zn-Ba-Cu-Fe deposits; and 9, Fe-Cu sulfides under Fe-Mn crusts.

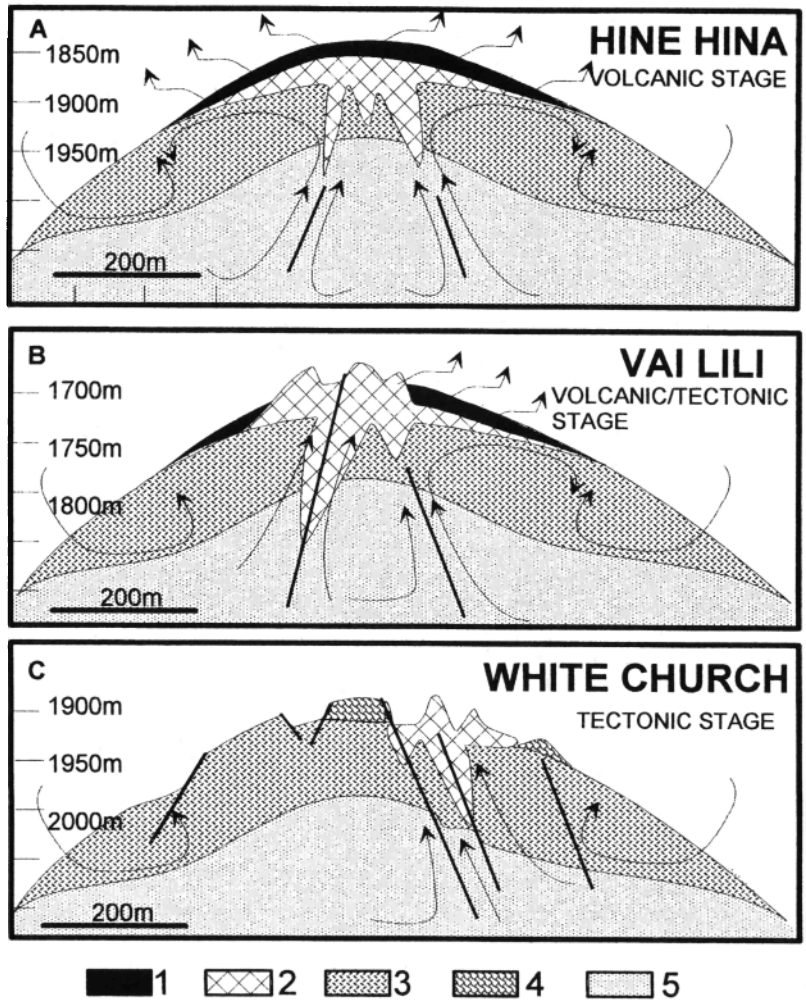


**Figure 2.** Schematic vertical section across the three main hydrothermal deposits of the Valu Fa Ridge. This illustrates from south to north the changes in the hydrothermal discharge and morphology of deposits in relation to tectonic activity versus volcanic activity (see text). 1, Fe/Mn crust and sulfide impregnation in volcaniclastic material (thickness not to scale); 2, massive sulfides; 3, brecciated andesite; 4, pillow lava field; and 5, massive andesite.

hydrothermal deposit in the Lau basin is apparently controlled by the type of volcanism and by tectonic activity, which increases from south to north. During the volcanic stage (Hine Hina field), diffuse discharge through highly porous volcaniclastic material produces extensive Fe/Mn oxide crusts covering sulfide deposits within the volcanic material. During the second stage (Vai Lili field), tectonic activity increases and more focused fault-controlled discharge forms chimneys on the seafloor. Diffuse discharge is still present, however. During the third stage (White Church field), hydrothermal activity is completely controlled by major faults and results in the development of sulfide mounds.

**2.2.1. Hine Hina hydrothermal field (southern Valu Fa Ridge).** Hine Hina is a 2 km long bathymetric high, up to 1820 m water depth, characterized by widespread low-temperature (40°C) hydrothermal activity. The outcrop is capped by a Fe-Mn crust, pierced by 13 brown inactive nodular chimneys up to 2 m high, composed of barite and Fe-poor sphalerite, with minor Pb-As sulfides and sulfo-salts. Under the crust, bleached volcanic and volcaniclastic rocks are the host for massive Fe-Cu sulfides (pyrite and marcasite, with decimetric channel-like coatings of chalcopyrite).

The Fe-Mn crust covering the area represents a first stage of hydrothermal activity (broad discharge through permeable vesicular and brecciated basaltic andesites), leading progressively to a near-surface sealing of the hydrothermal system. This cap prevented any subsequent substantial mixing with seawater and resulted in intensive subsurface alteration of the volcanics by circulating higher temperature hydrothermal fluids. These higher temperature fluids circulated laterally below the hardened sediments, causing massive Cu-Fe sulfides to precipitate as horizontal layers beneath the crust. Locally, Ba-Zn chimneys are formed on top of the sediment.

**2.2.2. Vai Lili hydrothermal field (central Valu Fa Ridge ).** This field, 400 m long and 100 m wide, in 1720 m of water, is directly related to N-S trending normal faults with up to 15 m vertical offset. It is characterized by numerous venting chimneys, both white and black smokers (up to 400°C), and the presence of sulfide mounds. At the scarp of the N-S trending fault, a complete cross section exhibits

the following sequence, from top to bottom: (1) Ca-(Ba)-Cu chimneys (black smokers), with chalcopyrite and barite, together with anhydrite in active vents; (2) Ba-Zn chimneys (white smokers), precipitating directly barite, sphalerite, and galena in contact with seawater, in the active vents; locally, tennantite is particularly abundant and associated with primary bornite; grains of primary native gold were found in sphalerite and more rarely in tennantite [*Herzig et al.*, 1993]; (3) massive Zn-Ba sulfides; (4) massive Cu sulfides, with mainly chalcopyrite, and subordinated pyrite (early), associated with marcasite; sphalerite is rare; barite is scarce and, in contrast to samples from the top of the deposit, occurs as a late mineral; (5) a stockwork, with two generations of veins: the first, filled with pyrite and chalcopyrite, and minor sphalerite and tennantite; the second, filled with coarse-grained barite, associated with pyrite, sphalerite and galena.

Because of the active normal faulting, both focused hydrothermal discharge along the normal fault and diffuse discharge associated with Mn-Fe precipitates are present at the site. Thus sulfides form within the volcaniclastics and also occur as chimneys and mineralogically zoned massive sulfide mounds on the seafloor. At the same time, a stockwork is forming along the faults.

**2.2.3. White Church field (northern Valu Fa Ridge ).** The large inactive hydrothermal White Church site is located on the upper eastern flank of the northern Valu Fa Ridge, at water depths between 1966 and 1946 m. The field extends over 300 m, following the foot of a ridge-parallel, 60 m high, normal fault. Three types of mineral deposits are observed: (1) barite chimneys, with early dendritic barite (with pyrite inclusions), followed by sphalerite, galena and minor tennantite, and a late coarse-grained barite, associated with amorphous silica; (2) impregnation of the altered andesite by barite, as tabular idiomorphic crystals, and subordinated various sulfides: idiomorphic pyrite or marcasite (millimeter-sized), with epitaxic growth of galena and sphalerite, chalcopyrite grains with epitaxial galena, pyrrhotite, filling the vesicles of the andesite; and (3) a massive sulfide talus in the vicinity of the chimneys, with mainly chalcopyrite, associated with sphalerite and rare opal.

Here, the tectonic control on hydrothermal activity is even more pronounced than at Vai Lili. Near the hydrothermal field, whose location is controlled by a major fault, there is no evidence for widespread Mn-Fe deposits. On the contrary, the distribution of Mn chimneys is controlled by faults, indicating the importance of fault control on even low temperature discharges. The sulfides occur both as Ba-Zn chimneys and massive sulfides on the seafloor. However, the presence of hydrothermally cemented volcanic breccia suggests that important sulfide precipitation occurs within the oceanic crust and probably in stockworks rooted in the fault underneath.

## 3. Analytical Methods and Samples

### 3.1. Fluid Inclusion Studies

Fluid inclusions were studied in doubly-polished 200 μm thick wafers. The wafers were prepared with special care in order to prevent stretching of the fluid inclusions in barite and anhydrite. Microthermometric observations were carried out using a Fluid Inc. adapted U.S. Geological Survey (USGS)-type heating/freezing stage, calibrated with synthetic fluid inclusions (pure water: ice melting temperature of 0.0°C and critical homogenization temperature of 374.1°C; pure $CO_2$-water inclusions: $CO_2$ melting temperature of -56.6°C). Fluid inclusions in sphalerite were studied using a Chaix-Meca heating/freezing stage [*Poty et al.*, 1976], which allowed better visibility of the inclusions within the rather dark sphalerite crystals. The Chaix-Meca stage was calibrated using the same synthetic fluid inclusions as for the USGS stage. The rate of heating was monitored to obtain an accuracy of ±0.2°C during freezing runs and ±1°C when heating over the 25-400°C range (±3°C in sphalerite, due to the darkening of the mineral while heating). All reported measurements represent individual inclusions; as far as possible, ice melting and homogenization temperatures were measured in the same inclusions. The presence of volatiles within the vapor phase in the fluid inclusions was investigated by micro-Raman analysis, performed on a DILOR X-Y multichannel modular Raman spectrometer [*Dhamelincourt et al.*, 1979].

### 3.2. Strontium Isotopes in Sulfides and Sulfates

Sr isotopic analyses were performed at the University of Rennes. Sulfide and sulfate samples were purified by hand-picking and crushed in an agate mortar. About 50 mg of the resulting powders was dissolved using mixtures of perchloric and sulfuric acids (sulfates) and of fluorydric and hydrochlorydric acids (sulfides), and Sr was separated using cation-exchange chromatography. Total Sr in the blanks was less than 0.5 ng. Isotopic measurements were carried out using the Faraday cups of a five-collector Finnigan MAT 262 mass spectrometer. All measured $^{87}Sr/^{86}Sr$ ratios were normalized against $^{86}Sr/^{88}Sr = 0.1194$ to correct for isotopic fractionation effects. During the course of this study, 10 separate analyses of the standard National Bureau of Standards (NBS) 987 Sr yielded $^{87}Sr/^{86}Sr = 0.710236 \pm 0.000009$. Sr concentrations were determined by XRF spectrometry. Analytical uncertainties are ±1% for concentrations ≥1000 ppm and ± 10% for concentrations ≤10 ppm.

### 3.3. Oxygen Isotopes of Water Inclusions Trapped in Sulfides and Sulfates

Fluid inclusions trapped in marcasite, chalcopyrite, sphalerite, and barite were extracted under vacuum by thermal decrepitation. Samples weighing from 500 mg to 5 g were degassed at 50°C for a minimum of 2 hours under vacuum. The samples were then thermally decrepitated, and $H_2O$ collected in a trap held at liquid nitrogen temperature. Water was the only major gaseous phase detected during thermal decrepitation of both sulfides and sulfates, an observation in agreement with the microthermometric observations. Water, in the range 20-300 μmoles, was liberated during decrepitation. This $H_2O$ was then transferred to a microequilibration vessel to which 30-50 μmoles of $CO_2$ were added. The $H_2O$ and $CO_2$ of known amount and isotopic composition were then allowed to exchange oxygen isotopes at 30°C for 3 days. After this time, equilibration was complete, and the equilibrated samples of $H_2O$ and $CO_2$ were separated cryogenically once again. The $\delta^{18}O$ values of the water samples were calculated using the mass balance equation (1) of *Kishima and Sakai* [1980].

Table 1. Geochemical Measurements of Lau Basin Minerals and of Their Fluid Inclusions.

| Site | Mineral | Sample | Inclusions | Sr, ppm | $^{87}Sr/^{86}Sr$ | $H_2O$, ppm | $\delta^{18}O$ ($H_2O$) |
|---|---|---|---|---|---|---|---|
| Hine Hina | marcasite | NL1602 | trace barite | 10 | $0.704747\pm7\times10^{-6}$ | 100 | 0.7±0.3 |
| | marcasite | NL1602 | trace barite | 10 | $0.704747\pm7\times10^{-6}$ | 100 | 0.4±0.3 |
| | barite | NL1602 | - | 7000 | $0.704553\pm8\times10^{-6}$ | 200 | 2.2±0.2 |
| | chalcopyrite | NL1602 | ? | <10 | $0.706176\pm8\times10^{-6}$ | 1000 | 2.5±0.3 |
| Vai Lili | sphalerite | BL12 | anhydrite | 2000 | $0.707816\pm7\times10^{-6}$ | 50000 | 4.4±0.2 |
| | sphalerite | NL2206b | barite | 1300 | $0.705187\pm7\times10^{-6}$ | 1600 | 4.1±0.2 |

Strontium contents and isotopic compositions have been performed on bulk minerals, whereas oxygen isotope ratios (‰ SMOW) have been determined in water inclusions by thermal decrepitation. Water contents have been calculated on the basis of $H_2$ yields after reduction of water with zinc metal at 500°C

$$\delta^{18}O\,H_2O=\left(\delta^{18}O\,CO_2(f)-\delta^{18}O\,CO_2(i)\right)\left(2\frac{[CO_2]}{[H_2O]}\right)$$

$$+\left(1+\frac{\delta^{18}O\,CO_2(f)}{1000}\right)\frac{1000}{\alpha_{CO_2\text{-}H_2O}}-1000 \qquad (1)$$

with $\alpha$ $CO_2$-$H_2O$ = 1.0402 at T= 30°C [*O'Neil and Adami*, 1969], $\delta^{18}O$ $CO_2$ (f) = $\delta^{18}O$ of $CO_2$ equilibrated after 3 days with $H_2O$, $\delta^{18}O$ $CO_2$ (i) = $\delta^{18}O$ of $CO_2$ before equilibrium with $H_2O$ = 16.15±0.05 (SMOW), and $[CO_2]$ and $[H_2O]$ are the amounts of the two gases in µmoles. Precisions obtained during the experiments for $\delta^{18}O$ values of $H_2O$ were in the range 0.2‰ - 0.3‰ (Table 1) depending on the $CO_2/H_2O$ ratio during the equilibration procedure (Figure 3). Conditions of thermal decrepitation were adjusted for each sample. Heating rates did not exceed 50°C.min$^{-1}$, and peak temperatures remained below 500°C, to avoid a redox reaction between sulfide and water producing both sulfate and hydrogen. This reaction occurred during some of our experiments and was easily detectable. We observed an artificial $^{16}O$ enrichment of the residual water ($\delta^{18}O$ values down to -10‰) and anomalous low water yields that never exceeded 50%. Water yields are calculated on the basis of calibrated hydrogen pressure measured with the mass spectrometer gauge. Extraction and oxygen isotope measurement of the water included in sulfides from Lau have been successful for samples with water contents as low as 100 ppm (Table 1).

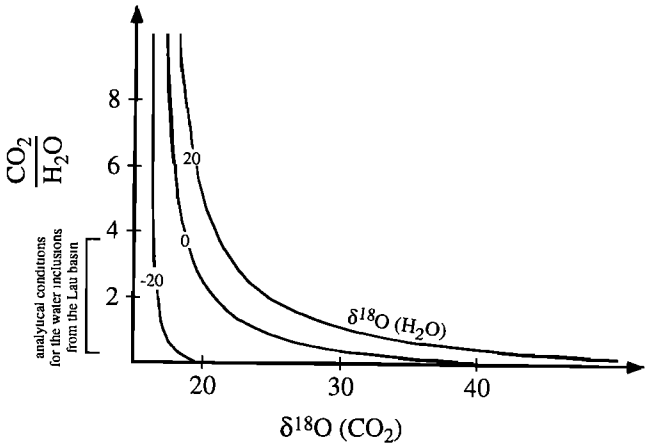


**Figure 3.** Curves for calculated $\delta^{18}O$ values of water inclusions as a function of the $CO_2/H_2O$ ratio and the $\delta^{18}O$ value of $CO_2$ during micro-equilibration experiments. A better precision in the determination of the $\delta^{18}O$ value of $H_2O$ is obtained in the domain of low $CO_2/H_2O$ ratios where the slope of the curves is slight.

### 3.4. Samples

Samples were collected during the *Nautilau* cruise in 1989 [*Fouquet et al.*, 1991a]. They come from the three main hydrothermal systems of the Valu Fa Ridge.

**3.4.1. Vai Lili.** Sample BL 12, collected at 1727 m water depth from a vigorously active black smoker (342°C), consists mainly of barite (outer part) and sphalerite, with an inner wall of chalcopyrite, and a coating of massive microcrystalline anhydrite, on this inner wall. Only anhydrite was found to contain fluid inclusions and was used for microthermometry. Sphalerite was used for isotope studies.

Sample NL 22 06 was collected beneath the chimneys, at 1735 m water depth, and consists of a conduit within the massive sulfides. It consists mainly of small barite crystals as interstitial cement in massive sulfides (chalcopyrite and sphalerite). Tennantite is common. Marcasite, opal, and galena are rare. Barite was used for microthermometry and sphalerite for isotope studies. No fluid inclusions were found in the sphalerite.

**3.4.2. Hine Hina.** Sample NL 16 02, collected at 1820 m water depth, is part of a massive marcasite body, with a late chalcopyrite channel, within the massive Fe-Cu sulfides formed as replacement of the volcaniclastic material. Marcasite is preferentially replaced by pyrite close to the chalcopyrite rim. Barite is also present, as idiomorphic crystals up to 1 cm long, together with minor sphalerite and pyrite, apparently as a late overgrowth on chalcopyrite or marcasite. Barite was used for microthermometric studies; barite, marcasite, and chalcopyrite were used for isotope studies.

Barite and chalcopyrite were examined in this sample using proton-induced X-ray emission (PIXE): barite contains Sr (7600±90 ppm), Fe (220±40 ppm) and Cu (120±5 ppm); chalcopyrite is rich in Co (1500±600 ppm) and Pb (1070±10 ppm).

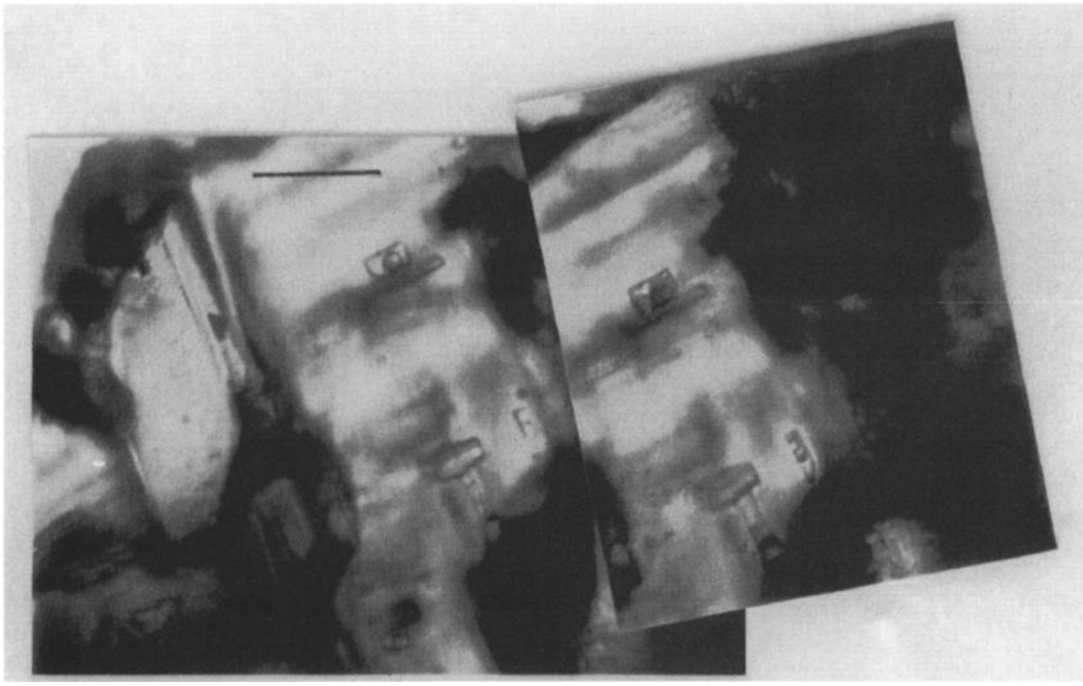

**Figure 4.** Photomicrograph of fluid inclusions in the anhydrite from sample BL 12 (Vai Lili field). The scale bar is 50 μm.

**3.4.3. White Church.** Sample NL 08 06, collected at 1960 m water depth, within the massive sulfide talus, consists of aggregates of large idiomorphic sphalerite crystals, cementing earlier pyrite. Sphalerite was used for microthermometric studies.

## 4. Results

### 4.1. Fluid inclusions

**4.1.1. Fluid inclusions in anhydrite (Vai Lili).** Anhydrite-hosted fluid inclusions are infrequent in the BL 12 sample. They are small (10-20 μm), display negative crystal (rectangular prism) shapes, and occur along two directions, parallel and orthogonal to the crystal elongation (Figure 4). Heating measurements on these inclusions were performed before freezing because most inclusions were damaged (leakage or decrepitation) during freezing due to the very brittle nature of anhydrite. In addition, in many inclusions, stretching-induced leakage was observed during heating, and temperature measurements had to be disregarded. Inclusions were measured in several crystals.

All inclusions are two-phase (L+V) at room temperature, with volume ratios of vapor (Rv) between 0.40 and 0.50. During freezing, systematic nucleation of halite was recorded and has been identified on the basis of cubic morphology, onset of nucleation, and isotropic character. No change in bubble size was observed after halite nucleation. It is thus suggested that halite oversaturation in these inclusions was metastable at room temperature in these inclusions, a rather uncommon situation, possibly due to quenching of the host mineral in this high-temperature chimney environment. Unfortunately, most inclusions were damaged upon freezing, and only two measurements of the melting temperature of halite could be performed. They are in a narrow range (127-134°C). Given the apparent consistency of the halite to liquid ratios in all inclusions, these values are thought to be representative of the salinity of the trapped fluid. Melting of halite occurred before the bulk homogenization of the inclusions in the liquid state. Only five measurements were retained in the range of 290-344°C.

There are several problems in interpreting fluid inclusion measurements in anhydrite [*Tivey et al.*, 1998; and references therein]. These include (1) stretching during heating, (2) partial dissolution of the anhydrite walls, (3) gypsum precipitation, (4) and anhydrite precipitation during heating. Gypsum precipitation is of special concern. In the anhydrite of the TAG hydrothermal deposit on the Mid-Atlantic Ridge, *Tivey et al.* [1998] observed that fine-grained (<1 μm) daughter crystals could nucleate in some fluid inclusions, following freezing and being left 12 hours at room temperature. These crystals were dissolved upon heating to 108-120°C. They are thought to be gypsum, resulting from reaction of the anhydrite walls with the trapped fluid [*Tivey et al.*, 1998]. Such daughter crystals cannot be compared with those nucleating in the BL 12 anhydrite that are larger and are considered to be halite on the basis of cubic morphology and isotropic behavior. Moreover, in the BL 12 inclusions, no melting of ice at temperatures below 0°C could be observed, indicating that we are effectively dealing with a NaCl-oversaturated system at room temperature. Other possible problems for anhydrite inclusions mainly concern changes in the volume of the inclusions, therefore affecting the homogenization temperatures. Although only five measurements were performed with the Vai Lili anhydrite, they seem consistent at the crystal scale, and therefore we believe that the perturbation effects on the homogenization temperatures are, at most, of limited extent.

Thus the microthermometric results in the Vai Lili anhydrite are considered meaningful. They indicate that the fluid inclusions contain a brine whose composition may be

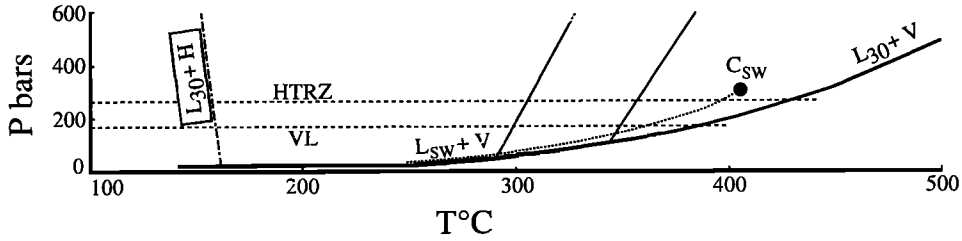


**Figure 5.** Isochores for the fluid inclusions in the anhydrite from the Vai Lili field (sample BL 12). $L_{30}$ +H is the liquid (30% NaCl) + halite curve, $L_{30}$ + V is the liquid (30% NaCl) + vapor curve, $L_{sw}$ + V is the liquid + vapor curve for seawater, $C_{sw}$ is the critical point for seawater. Isobar labeled HTRZ is the isobar at the HTRZ depth, and that labeled VL is the isobar at the seafloor depth at Vai Lili.

calculated from the melting temperature of halite by using the equations of *Sterner et al.* [1988] and assuming that the fluid may be approximated by the NaCl-$H_2O$ system. A high salinity close to 30 wt % eq NaCl is calculated (28.8% and 29.1% for melting temperatures of halite of 127°C and 134°C, respectively). This high salinity cannot be the result of anhydrite dissolution from the walls of the inclusions since the maximum increase in salinity by this mechanism would be 0.65 wt % eq NaCl [*Tivey et al.*, 1998]. The corresponding isochores were drawn using data from *Bodnar et al.* [1985] and *Bodnar* [1994], which allow a determination of the trapping temperature of the fluid (at the 1727 m depth of the sample) between 300 and 350°C (Figure 5). These estimates are consistent with the present-day temperature at the vent (342°C [*Fouquet et al.*, 1993]), although present-day venting fluids at Vai Lili are far less saline (up to 4.7 wt % eq NaCl, [*Fouquet et al.*, 1991a, b]).

**4.1.2. Fluid inclusions in barite (Hine Hina and Vai Lili ).** In sample NL 16 02 of Hine Hina, detailed microthermometric investigations were made on one of the large barite crystals. Two types of fluid inclusions are observed. Type 1 are large (30-50 μm), irregular, two-phase (L+V) inclusions with rather low Rv (Table 2) either isolated or distributed in small clusters and systematically in the vicinity of pyrite solid inclusions in the barite (Figure 6a). These type 1 inclusions are thought to be primaries. Two sets of type 1 inclusions were considered, one close to the base of the crystal, the other close to the top of the crystal. Type 2 are small (5-10 μm) secondary two-phase (L+V) inclusions with rather low Rv (Table 2) that are trapped in healed microcracks (Figure 6b). These microcracks locally overprint type 1 inclusions. Both types yield similar microthermometric results (Figures 7a and 7b and Table 2): low first-melting temperature (Te) around -35°C, final melting temperature of ice (Tm ice) between -2.8 and -1.8°C, bulk homogenization temperatures in the liquid phase (Th(L)) in the 160-220°C range. Using a sequential freezing procedure as described by *Haynes* [1985], more detailed results were obtained in type 1 inclusions; first melting was accurately measured at -35°C, and the melting of rounded birefringent hydrohalite crystals was measured in the range -24.3 to -22.5°C. Due to the small size of type 2 inclusions, the observation of hydrohalite melting was not possible.

Precise determination of the eutectic temperature of -35°C

Table 2. Microthermometric Measurements in Fluid Inclusions From the Lau Basin.

| Sample | Support | Type | Rv | Te | Tmhy | Tmi | Tmh | Th(L) |
|---|---|---|---|---|---|---|---|---|
| Hine Hina | | | | | | | | |
| NL 16 02 | Bar | primary | 0.15-0.20 | -35 | -24.3/-22.5 | -2.8/-1.8 | | 177/219 |
| | | secondary | | -36/-34 | | -2.8/-2.0 | | 160/220 |
| Vai Lili | | | | | | | | |
| BL 12 | Anh | primary | 0.40/0.50 | | | * | 127/134† | 290/335 |
| NL 22 06 | Bar | primary | 0.15/0.20 | | | -1.5/-0 9 | | 180/200 |
| | | secondary | | | | | | 148/261 |
| Whitechurch | | | | | | | | |
| NL 08 06 | Sp | core | 0.20 | -21.8‡ | | -3.0/-2.6 | | 203/235 |
| | | rim | 0.20 | | | -3.2/-1.9 | | 253/262 |

Temperatures are in °C. Rv, volumic ratio of vapor content; Te, eutectic temperature; Tmhy, melting temperature of hydrohalite; Tmi, melting temperature of ice; Tmh, melting temperature of halite; Th(L), bulk homogenization temperature in the liquid state; Anh, anhydrite; Bar, barite; Sp, sphalerite

* Nucleation of a halite cube during freezing.

† Only two measurements.

‡ Only one measurement.

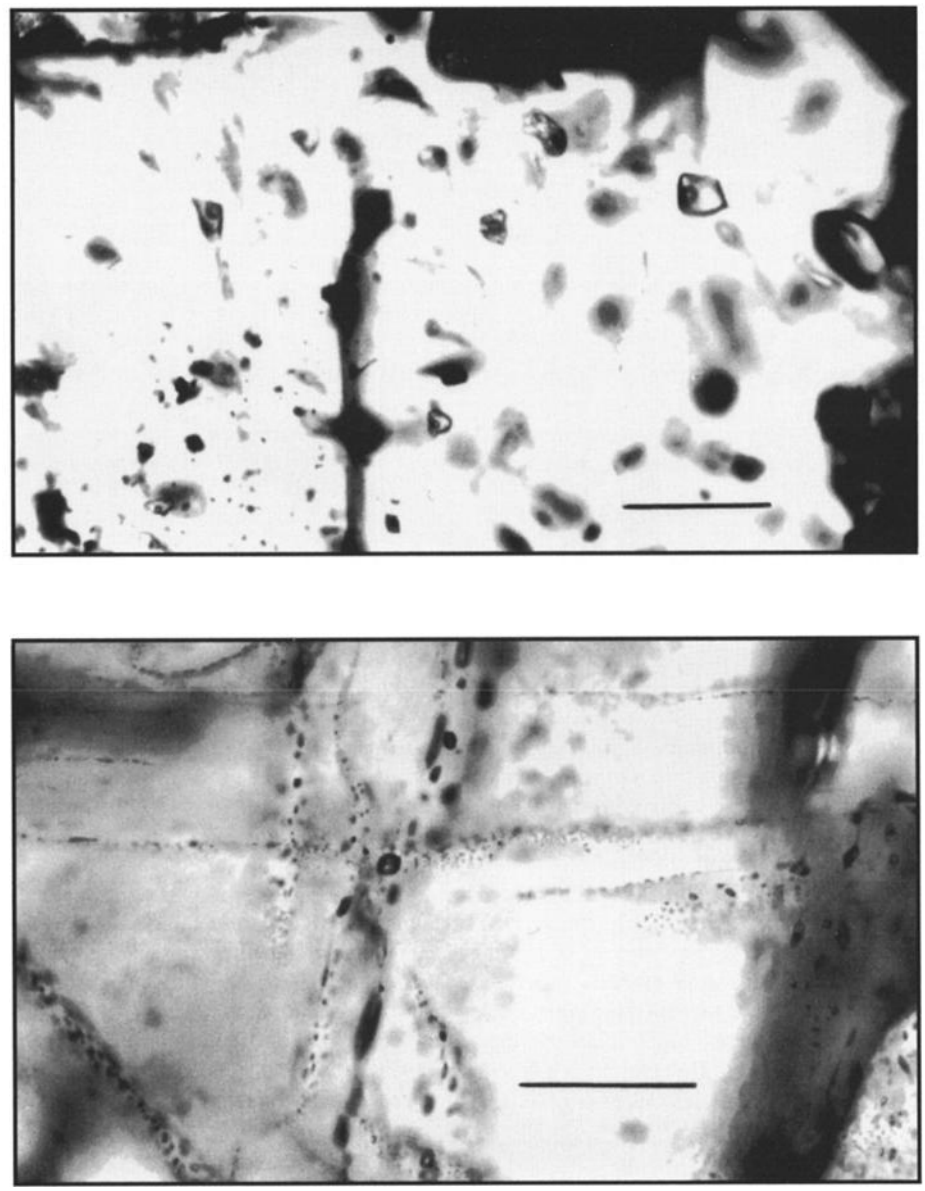


**Figure 6.** Photomicrographs of fluid inclusions in the coarse-grained barite from sample NL 16 02 (Hine Hina field): (a) cluster of large inclusions in barite clouded with pyrite inclusions (black specks); the scale bar is 100 μm; and (b) planes of secondary fluid inclusions; the scale bar is 100 μm.

in the primary inclusions of the barite at Hine Hina (NL 16 02 sample) is strong evidence that the fluid trapped in the barite crystals was a member of the $H_2O$-NaCl-$MgCl_2$ system [*Crawford*, 1981]. Should this fluid have significant content of $CaCl_2$ (as would be the case of seawater), the eutectic should be depressed at -52°C [*Vanko et al.*, 1988]. The $H_2O$-NaCl-$MgCl_2$ system was recently described by *Dubois and Marignac* [1997], which allows determination of the fluid composition using the melting temperatures of hydrohalite and ice (Figure 8). Using the data of *Zhang and Frantz* [1987], isochores may be calculated, and a pressure correction of 10°C is estimated for the 1900 m depth of the Hine Hina sample. Thus the trapping temperatures, which are recorded by the fluid inclusions in the barite, span the 170-230°C range (Figure 9). This procedure is valid, since the isochores for the different salt-water systems are very close each other for a given Th(L) [*Zhang and Frantz* , 1987].

In sample NL 22 06 of Vai Lili, two types of inclusions are observed in the barite: (1) isolated two-phase (L+V) inclusions that are considered as primaries and characterized by high Tm ice (-1.5 to -0.9°C) and Th(L) close to 190°C (Figure 7c and Table 2); (2) clusters of very small, most often one-phase (L) inclusions; some of them, however, are two-phase (L+V) inclusions, displaying variable Th(L) in the 148 to 261°C range (Figure 7c); it was not possible to measure the Tm ice.

From the equation of *Bodnar* [1993], salinities of 1.6 to 2.6 wt % eq NaCl are calculated. Using the data of *Zhang and*

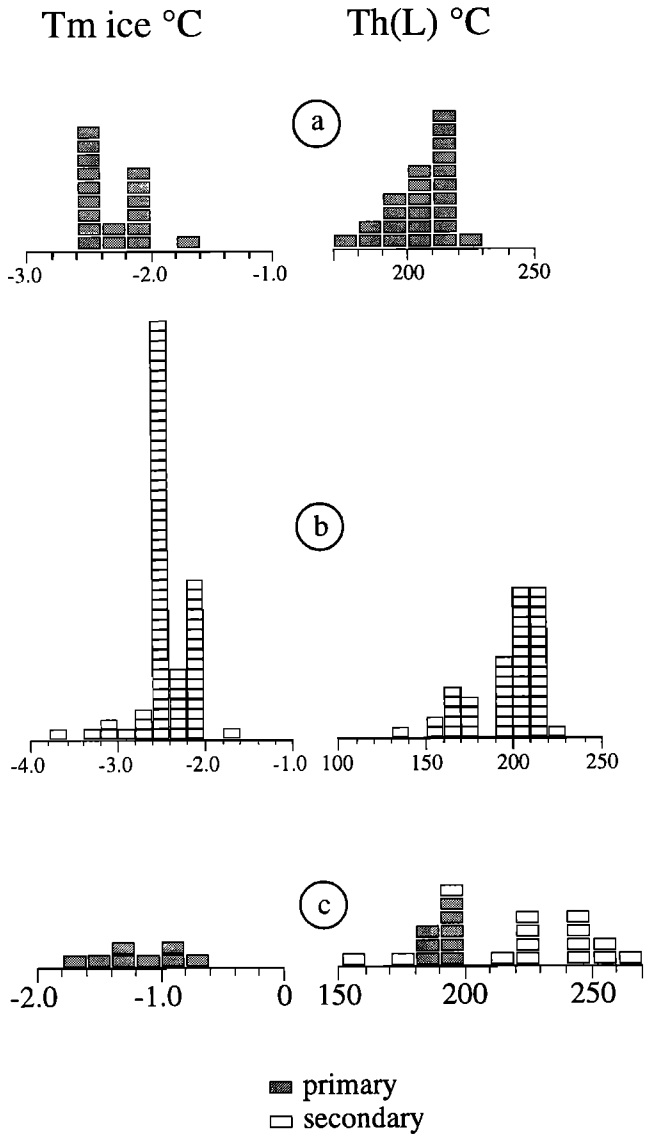


**Figure 7.** Histograms of temperature measurements (Tm ice and Th(L)) for fluid inclusions in the barites from the Lau basin. (a, b) Barite from the Hine Hina field (sample NL 16 02) showing (a) primary inclusions, and (b) secondary inclusions, and (c) barite from the Vai Lili field (sample NL 22 06).

*Frantz* [1987], isochores may be calculated, and the trapping temperatures of these fluids at the 1735 m water depth of the sample are estimated at ≈ 200°C (Figure 9).

**4.1.3. Fluid inclusions in sphalerite (White Church).** In sample NL 08 06 the large idiomorphic sphalerite crystals display a consistent zonation pattern with a red to orange core and a yellow rim. Fluid inclusions are present in both zones as very small (≤10 μm) two-phase (L+V) inclusions either oval in shape or displaying negative crystal (tetrahedral) morphology. They occur either isolated (probably, primary inclusions) or in healed microcracks of very short extension (pseudosecondaries [*Roedder*, 1984]) (Figure 10). Te could be measured in only two inclusions (-20.8 and -22.3°C). Final melting of ice occurs at similar temperatures in both zones in the -3.2 to -1.9°C range. Homogenization temperatures (Th(L)), although rather constant in a given zone, display systematic differences between core and rim, with lower temperature inclusions in the cores (203-235°C) as compared to the rims (253-262°C) (Table 2 and Figure 11). The Th(L) dispersion in the cores is possibly due to minor necking-down effects (see Figure 10b), but small temperature variations at the vent cannot be excluded.

From the measured eutectic temperatures close to -21°C, it can be concluded that the fluids trapped in the sphalerite of sample NL 08 06 may be approximated by the $H_2O$-NaCl system. Using the melting temperature of ice and the data of *Bodnar* [1993], salinities of 3.2 to 5.3 wt % eq NaCl are calculated. Using the data of *Zhang and Frantz* [1987], isochores may be drawn and yield a pressure correction of 10°C for the 1950 m depth of the White Church sample (Figure 9).

**4.1.4. Raman investigations.** Two inclusions, one (NL 08 06/6) from a sphalerite crystal, the other (NL 16 02-g/1) from a barite crystal were examined by micro-Raman spectrometry. No volatile component ($CO_2$, $CH_4$, $N_2$, $H_2S$) could be detected at the detection limit of the apparatus, i.e., $10^{-2}$ mole for $CO_2$ and $N_2$ and $10^{-3}$ mole for $CH_4$ and $H_2S$.

### 4.2. Strontium Isotopes

Table 1 reports $^{87}Sr/^{86}Sr$ ratios for Valu Fa Ridge sulfate and sulfide minerals (Hine Hina and Vai Lili fields). Although sulfide samples were carefully hand-picked, Sr contents are still such (2000 and 1300 ppm in sphalerite samples BL 12 and NL 22 06b, respectively) that most of the Sr in these samples must be controlled by inclusions of minute sulfate crystals in which Sr is substituted for Ca (anhydrite) or Ba (barite). In hydrothermal deposits from the East Pacific Rise at 21°N, *Albarède et al.* [1981] have made similar observations and demonstrated that Sr was not incorporated in the sphalerite structure. The two sulfate minerals contain varying

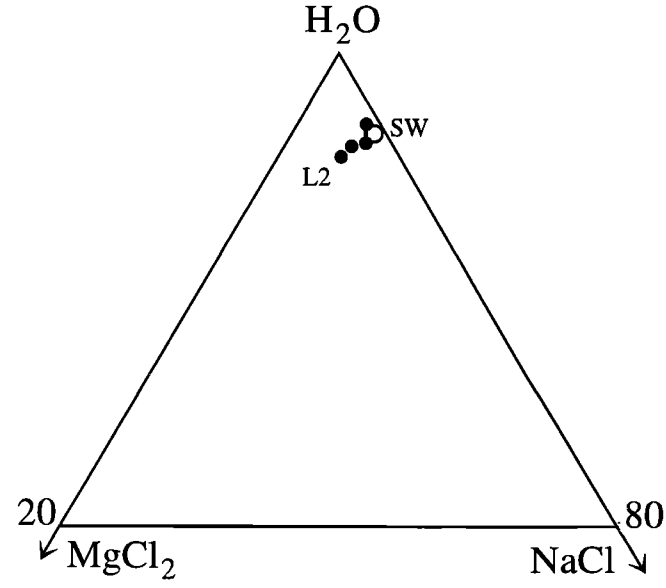


**Figure 8.** Plot of the fluid composition for primary fluid inclusions in barites from Hine Hina using the model system $H_2O$-NaCl-$MgCl_2$ [adapted from *Dubois and Marignac*, 1997]. SW is seawater composition, plotted from the microthermometric data of *Fujino et al.* [1974]. L2 is hydrothermal end-member (see text).

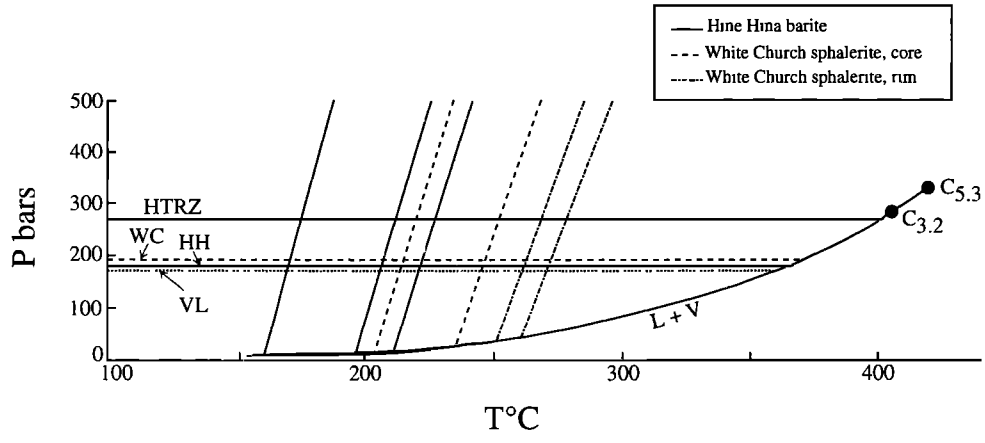


**Figure 9.** Isochores for the fluid inclusions in barite from the Hine Hina field and in sphalerite from the White Church field. L + V is the liquid-vapor curve for the $H_2O$-3.2% NaCl (= seawater) and the $H_2O$-5.3% NaCl (= saline fluid in sphalerite) systems (the two curves cannot be separated at the scale of the figure). C3.2 is the critical point (3.2% NaCl), and C5.3 is the critical point (5.3% NaCl). HH is the seafloor isobar at Hine Hina, HTRZ the isobar of the HTRZ, VL the seafloor isobar at Vai Lili, and WC the seafloor isobar at White Church.

amounts of Sr (Table 1) whose source may be either the andesitic basement or seawater. At Hine Hina, barite inclusions in marcasite have a $^{87}Sr/^{86}Sr$ value of 0.7047 similar to coarse-grained barite ($^{87}Sr/^{86}Sr$ = 0.7045) that constitute composite chimneys and which contain about 7000 ppm of Sr. Sulfate trace inclusions in the chalcopyrite of these composite chimneys have a high $^{87}Sr/^{86}Sr$ ratio of 0.7062. At Vai Lili, anhydrite inclusions in sphalerite from sample BL 12 have a high $^{87}Sr/^{86}Sr$ ratio of 0.7078 in comparison to the low value of 0.7052 found for barite inclusions in sphalerite from NL 22 06 sample. It is worth noting that all the samples have $^{87}Sr/^{86}Sr$ ratios intermediate between that of pure seawater (0.7091) and the value of 0.7044 obtained for the Valu Fa Ridge venting hydrothermal waters.

### 4.3. Oxygen Isotopes

Oxygen isotope compositions of aqueous inclusions have been measured in the same samples studied for Sr isotope ratios. Assuming that no fractionation occurred during trapping of the fluids, the $\delta^{18}O$ values of these aqueous inclusions may be considered to be those of hydrothermal fluids circulating in the crust at the time of chimney formation. For both the Hine Hina and Vai Lili fields, the $\delta^{18}O$ values of aqueous inclusions trapped in sulfides and barite range from 0.4 to 4.4‰. At Hine Hina (sample NL 16 02), the $\delta^{18}O$ value of hydrothermal water trapped in marcasite is close to 0.5‰, a value slightly higher than the pure seawater end-member ($\delta^{18}O$ = 0‰). In the same sample, hydrothermal waters that precipitated either chalcopyrite or barite crystals have $\delta^{18}O$ values of 2.5 and 2.2‰, respectively. At Vai Lili, sphalerite crystals from two different chimneys (samples NL 22 06b and BL 12) contain hydrothermal waters that have the highest $\delta^{18}O$ values of 4.1 and 4.4‰.

The significance of oxygen isotope composition of fluid inclusions in barite must be questioned because it could be suspected that these fluids were isotopically reequilibrated with the host mineral during cooling. However, we think that in the Lau basin context, reequilibration of the fluids trapped within barite is unlikely because the $SO_4$ groups are characterized by a high activation energy [*Chiba and Sakai*, 1985]. Moreover, a quick cooling of the barite cannot be excluded, hence limiting the possibility of significant isotopic exchange with $H_2O$.

## 5. Discussion

### 5.1. Summary of Major Observations

We underline the most striking observations that will require the discussion of physical and chemical processes that may operate in the Lau basin hydrothermal system:

1. The presence in BL 12 anhydrite, inside a venting chimney, of preserved fluids with salinity of about 30 wt % eq NaCl is the first evidence that high-salinity brines may reach the seafloor in oceanic hydrothermal systems. By contrast, the fluids in the barite sample (NL 22 06) are characterized by low salinities. These salinities are lower than the salinity of seawater (3.2 wt % eq NaCl [*Bischoff and Rosenbauer*, 1984]).

2. The unusual documentation of Mg-bearing hydrothermal fluids with significant salinity variations in the barite sample (NL 16 02) of the Hine Hina chimney.

3. The salinities of aqueous fluids in the White Church sphalerite which are much higher (5.5 wt % NaCl) than that of seawater.

4. The first evidence of hydrothermal fluids with $\delta^{18}O$ values exceeding 4‰ in oceanic systems.

5. A large spectrum of $^{87}Sr/^{86}Sr$ ratios in anhydrite and barite that suggests various mixing ratios between Sr derived from seawater and from a magmatic source.

### 5.2. Hydrothermal and Magmatic Processes: Geochemical Implications

In a global frame of oceanic hydrothermal activity, we are potentially dealing with three types of fluids: seawater, evolved seawater (common hydrothermal end-member), and magmatic water. The magmatic water must be especially considered in the case of the Lau basin since the presence of silicic magmas may provide significant amounts of water compared to MOR magmas. In addition to mixing with

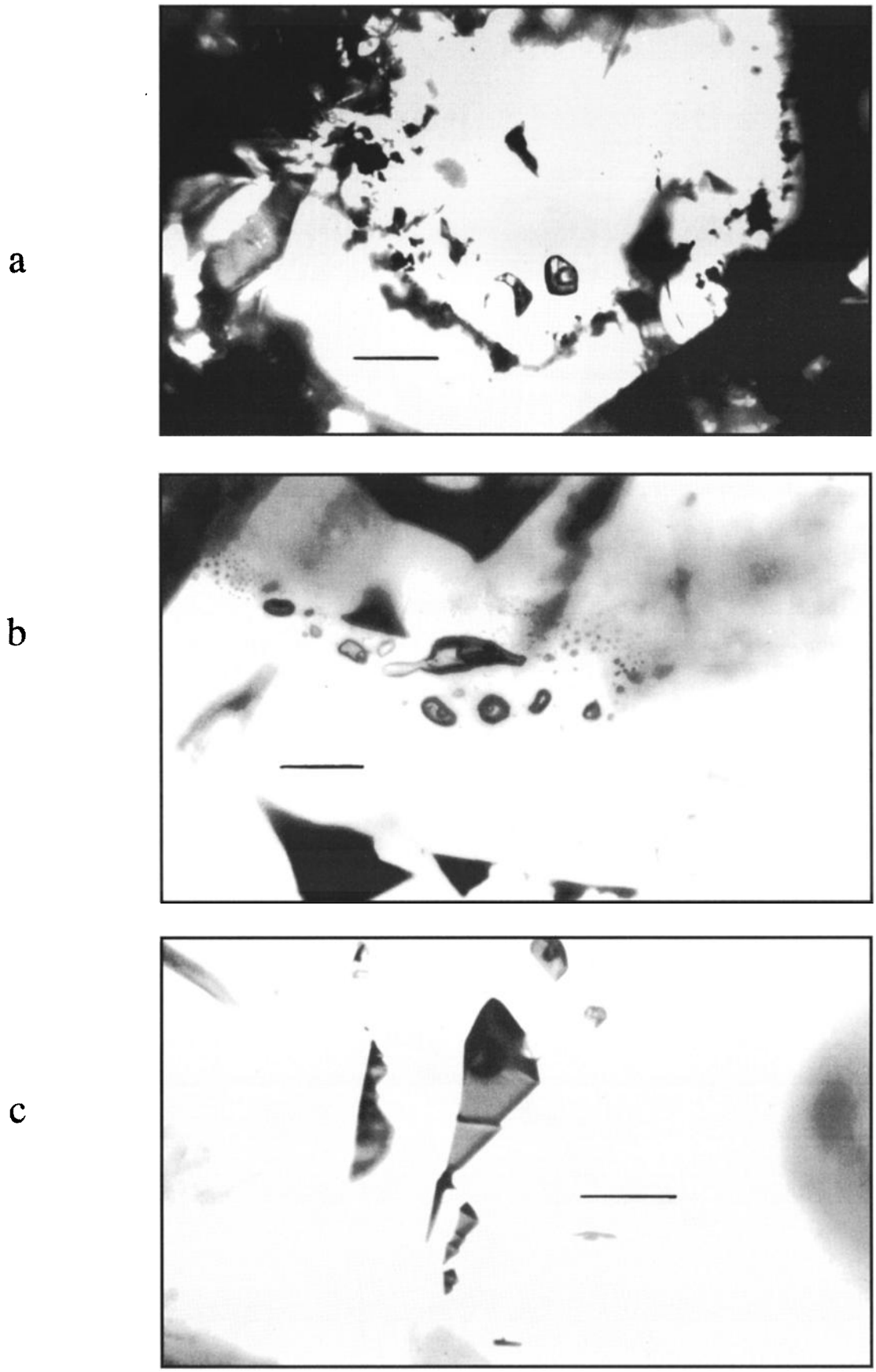


**Figure 10.** Photomicrographs of fluid inclusions in the zoned sphalerites from sample NL 08 06 (White Church field). (a) Isolated inclusions in the core of a zoned crystal (black specks are pyrite), the scale bar is 25 μm. (b) Cluster of pseudo-secondary inclusions, close to the boundary between core and rim of a zoned crystal (underlined by pyrite, in black); the scale bar is 25 μm. (c) Isolated inclusions with negative crystal morphology; the scale bar is 10 μm.

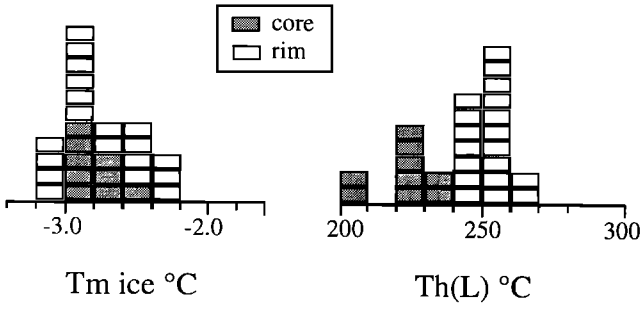


**Figure 11.** Histograms of temperature measurements (Tm ice and Th(L)) in fluid inclusions from sphalerite in the White Church field (sample NL 08 06).

seawater, processes that may affect fluid salinities and isotopic compositions are phase separation, contribution from a magmatic component, and fluid-rock interactions.

**5.2.1. Phase separation.** Phase separation is a suitable process to explain NaCl enrichment in hydrothermal fluids compared to seawater. The phase separation process in the $H_2O$-NaCl system, especially for seawater composition, has been discussed in many papers [e.g., *Bischoff and Pitzer*, 1985; *Delaney et al.*, 1987; *Goldfarb and Delaney*, 1988; *Butterfield et al.*, 1990; *Nehlig*, 1993; *Lowell et al.*, 1995]. Most workers emphasize the difference for seawater between subcritical boiling, yielding at the beginning a low-salinity vapor and a liquid with salinity close to that of seawater, from a dense fluid (a "liquid"); and supercritical condensation (also called supercritical phase separation), yielding at the beginning a moderately saline liquid and a vapor with salinity close to that of seawater, from an expanded fluid (a "vapor"). This is because subcritical phase separation is considered unable to yield high-salinity brines (more than twice the salinity of seawater) under the P-T conditions prevailing in many subseafloor hydrothermal systems [*Hedenquist*, 1984].

Phase separation is initiated when the seawater path intersects the (L+V) surface, or $(L+V)_{SW}$ curve in a P-T section (Figure 12), of the $H_2O$-NaCl system for seawater composition (3.2 wt % eq NaCl). In order to yield brines, this path must further intersect the (L+V) curves for higher salinities (Figure 12). This may be achieved by three ways as follows.

**5.2.1.1. Adiabatic phase separation:** It is generally assumed that seawater is upflowing along an adiabatic (isentropic) path [*Bischoff*, 1980; *Bischoff and Pitzer*, 1985; *Delaney et al.*, 1987]. When one of these paths intersects the (L+V) surface, phase separation occurs and the path is modified in the two-phase region, being nearly parallel to the immiscibility surface [*Bischoff and Pitzer*, 1985]. This is a major constraint on the possibility of getting brines. For instance, as seen in Figure 12, a fluid that intersects the $(L+V)_{SW}$ surface at 395°C, at the depth of the HTRZ in the Vai Lili field, could not intersect the $(L+V)_{30}$ surface before reaching the seafloor, at a depth of 1700 m. There, at a pressure of 170 bars and a temperature of ≈360°C (point A), it could finally intersect the $(L+V)_{15}$ curve, yielding a 15 wt % NaCl brine (using the isotherms of the $H_2O$-NaCl system from *Bischoff and Pitzer* [1989]). By the same way, considering a hotter fluid that intersects, for instance, the

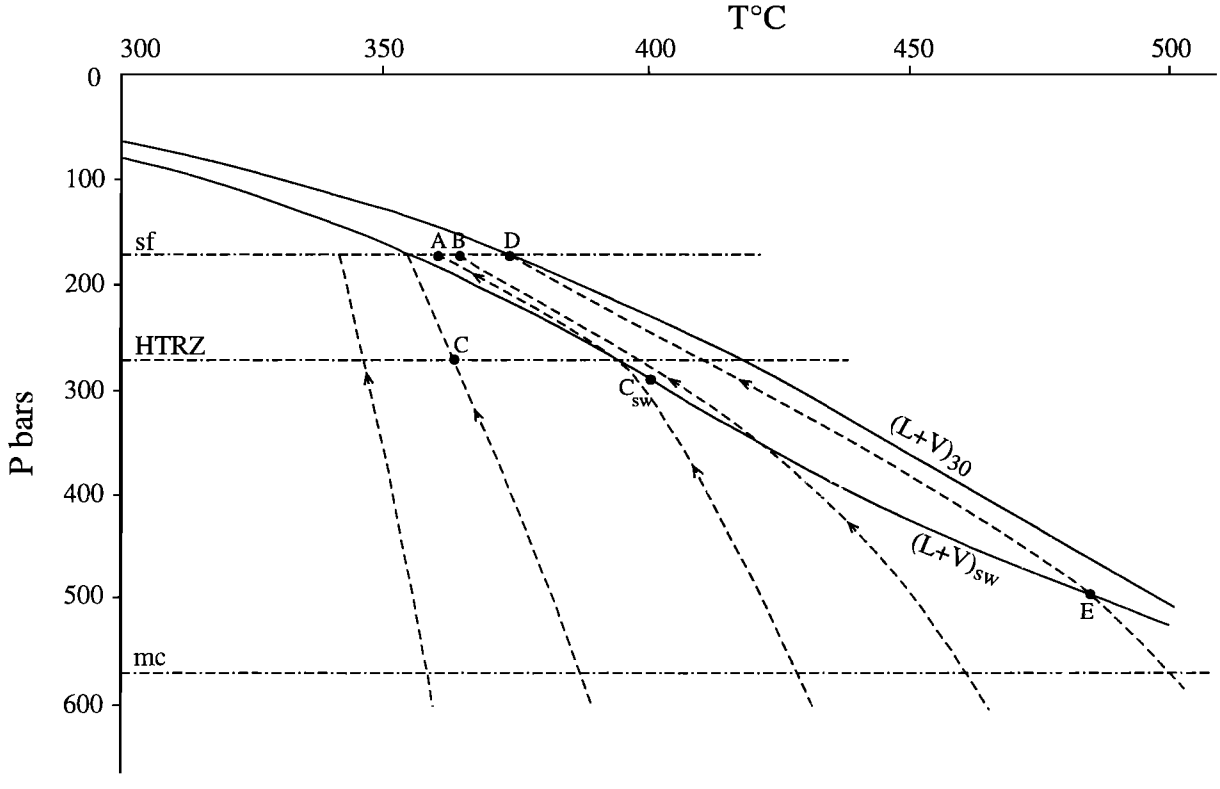


**Figure 12.** P-T projection for part of the $H_2O$-NaCl system, showing the conditions for seawater phase separation in the Vai Lili hydrothermal system (see text). Isobars are labeled sf at the seafloor (170 bars); HTRZ at the estimated 1 km depth of the HTRZ, assuming hydrostatic pressure gradients (see text); and mc at the estimated depth of the underlying magmatic chamber. The (L+V) curves for seawater ($(L+V)_{sw}$) and 30% NaCl ($(L+V)_{30}$) were constructed using data of *Bischoff and Pitzer* [1989]; $C_{sw}$ is the critical point for seawater.

$(L+V)_{sw}$ curve at 420°C and 350 bars (supercritical phase separation), finally it would only be possible to get a ≈20 wt % NaCl fluid close to the seafloor level (Figure 12, point B).

**5.2.1.2. Isobaric heating:** It is seen in Figure 12 that at a given depth below the seafloor, a temperature increase of ≈30-40°C is able to yield a brine up to 30% NaCl from initial seawater. For instance, at the depth of the HTRZ in the Vai Lili field, starting from seawater heated at 380°C, an increase of 40°C would correspond to the intersection with the $(L+V)_{30}$ curve at 420°C. Such a mechanism implies the existence of a more or less transient heat source, which is reasonably associated with the underlying magmatic activity underneath. A renewal of the magmatic activity (possibly as intrusion of small batches of acid magmas at a shallow level) would lead to heat transfer (conductive or advective) in the overlying reservoir. It is thought that the residence time of fluids in the HTRZ of mid-oceanic systems is of the order of several years (up to 20 years [*Butterfield et al.*, 1990, and references therein] that provides sufficient time for the above described process.

**5.2.1.3. Isothermal decompression:** As pointed by *Goldfarb and Delaney* [1988], fluid-rock interactions may lead to mineral deposition and sealing of cracks, thus yielding the possibility of fluctuating pressures in deep portions of the hydrothermal systems, even in the brittle part of the oceanic crust. Rapid transition from suprahydrostatic (up to lithostatic) to hydrostatic pressures could generate the conditions for phase separation. At the HTRZ depth in the Vai Lili field, Figure 12 shows that this could be achieved at a temperature of 395°C or more. However, to produce a 30 wt % NaCl brine, temperatures higher than 420°C are required. In the same way, at a 500 m depth, phase separation would be possible by this process at a temperature of ≈380°C or more, but temperatures higher than ≈410°C would be required to produce a 30 wt % NaCl brine. Therefore it is clear that in order to get brines, this process implies the existence of very high permanent temperature gradients compared to the process described above (section 5.2.1.2), which only requires transient high temperature gradients.

The phase separation process may also explain the $^{18}O$ enrichment in hydrothermal fluids. Indeed, thermodynamic data for the oxygen isotope fractionations between $H_2O(l)$ and $H_2O(v)$ in NaCl solutions at temperatures in the range 200-300°C predict that liquid water has $\delta^{18}O$ values 1‰ to 2.5‰ higher than vapor water [*Horita et al.*, 1995]. Yet, this enrichment is limited compared to the measured values in the Lau Basin.

**5.2.2. Contribution of magmatic fluids.** A high-salinity brine may be evolved in the subseafloor environment from water exsolved from a magmatic chamber [*Nehlig*, 1993 and references therein]. In the Lau basin environment, the presence of silicic melts with high water contents under the Lau ridge is well documented [*Fouquet et al.*, 1991a]. As demonstrated by *Cline and Bodnar* [1991], at low pressure (≈0.5 kbar), water saturation is achieved in silicic melts as soon as the crystallization begins, resulting in the unmixing of a low-salinity fluid. Under the corresponding P-T conditions, this fluid is, in turn, immediately unmixed into a brine and a vapor, the latter making up to 99 vol.% of the unmixed fluids (supercritical phase separation). The brine is highly saline with NaCl contents of 30 wt % or more.

Such magmatic fluids are likely to be enriched in $^{18}O$ compared to SMOW. In particular, a condensed vapor of magmatic origin according to this process should be characterized by $\delta^{18}O$ values in the 7-8‰ range [*Sheppard*, 1986]. Thus magmatic fluids are able to explain the observed $^{18}O$ enrichments of fluids relatively to seawater in the Lau basin.

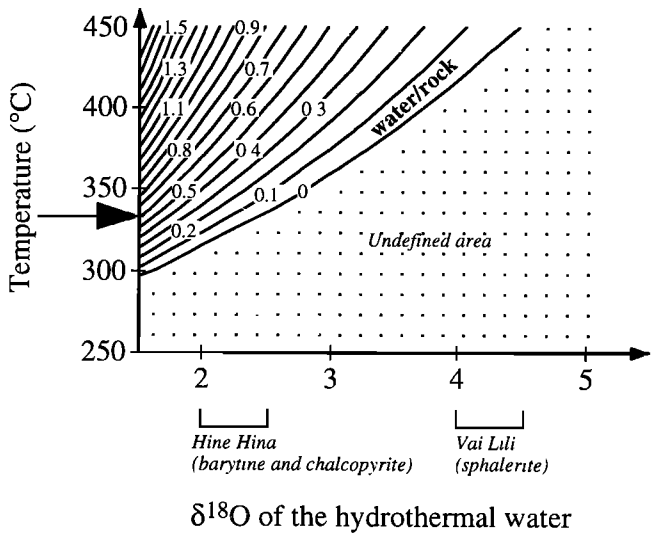


**Figure 13.** Domain of water-rock ratios defined by the temperature and oxygen isotope composition of hydrothermal fluids. The $\delta^{18}O$ values (‰ SMOW) of water inclusions that have been measured in the mineralizations from the Hine Hina and Vai Lili fields are reported.

**5.2.3. Fluid-rock interaction.** Variations of the $^{87}Sr/^{86}Sr$ ratios are readily explained by a mixing between seawater and the hydrothermal fluids whose strontium composition is either derived from the andesitic basement (0.7033-0.704 [*Loock et al.*, 1990]) by fluid-rock interaction or inherited from a magmatic source.

Concerning oxygen isotopes, the effects of water-rock interactions are commonly modeled using a time-integrated mass balance equation [*Taylor*, 1977] that assumes isotopic equilibrium between the total masses of interacting solid and liquid. The rock–water fractionation may be approximated by using the plagioclase–water fractionation given by the equation of *O'Neil and Taylor* [1967], as done previously by *Cocker et al.* [1982], *Schiffman et al.* [1984], and *Lécuyer and Fourcade* [1991] for studies of fossil hydrothermal systems preserved in ophiolites. Curves of equal water-rock ratios may be defined as a function of both temperature and oxygen isotope composition of the hydrothermal fluid (Figure 13). This kind of "box model" predicts $^{18}O$ enrichments of the hydrothermal end-members for water-rock ratios lower than 1 and temperatures higher than about 350°C (Figure 13). On the other hand, the chromatographic theory [e.g., *Baumgartner and Rumble*, 1988; *Fouillac and Javoy* , 1988; *Lassey and Blattner*, 1988] predicts the generation of $^{18}O$-rich hydrothermal fluids (up to 8‰) by fluid-rock interaction through the cumulative percolation of high-temperature fluids into a porous pile of magmatic rocks along a one-dimensional trajectory.

### 5.3. Application to Lau Basin Samples

Evidence for fluid mixing between seawater and hydrothermal end-members is described in this section.

**5.3.1. Importance of the mixing with seawater.** Sr isotope variations reflect various mixing ratios between seawater and hydrothermal end-members. Sr isotope compositions of coarse-grained barite crystals (Hine Hina NL 16 02) and inclusions in marcasite (Hine Hina NL 16 02) or sphalerite (Vai Lili NL 22 06b) have low $^{87}Sr/^{86}Sr$ ratios from 0.7045 to 0.7052 (Table 1). Thus these minerals were formed from a fluid dominated by the hydrothermal end-member. In contrast, higher $^{87}Sr/^{86}Sr$ ratios are encountered in the BL 12 Vai Lili sphalerite (0.7078 for anhydrite inclusions) and the Hine Hina chalcopyrite (0.7062 for anhydrite inclusions?). In these cases, the depositing fluids were more contaminated by seawater. In the absence of direct measurements of bulk Sr contents of the hydrothermal fluids, we cannot quantify the relative amounts of seawater and hydrothermal end-members in these minerals. It is interesting to note that *Fouquet et al.* [1993] estimated a mass fraction of 0.85 for the hydrothermal end-member in the present-day venting fluids of the Lau basin.

Consequently, the oxygen isotope composition of the hydrothermal end-member is likely higher than the highest $\delta^{18}O$ values of fluid inclusions measured in sphalerites from Vai Lili. Assuming the above mass fraction of 0.85 for the hydrothermal end-member, the $\delta^{18}O$ value is calculated as high as 5.2‰.

**5.3.2. Mixing of seawater with a NaCl-rich end-member (White Church sphalerite).** In the Th(L)-Tm ice diagram for fluid inclusions in the NL 08 06 sphalerite (Figure 14), two trends are identified. The first one corresponds to increasing Th(L) values from core to rim in a given crystal under a practically constant salinity (NL 08 06-6, Figure 14). We interpret this trend as an increase of the temperature of deposition during the sphalerite growth from 215-245°C in the cores to 260-270°C in the rims (Figure 9). A second trend is marked by a salinity change at a near-constant temperature in a given zone (NL 08 06-1, Figure 14). We interpret this second trend as a dilution trend that records an isothermal process of mixing between the hydrothermal end-member and a fluid of salinity close to that of seawater.

Thus, at White Church the hydrothermal end-member responsible for the sphalerite deposition (L1) is dominated by NaCl with a salinity of at least 5.5 wt % NaCl. This fluid is similar to the present-day venting fluids of the Vai Lili field, which is characterized by salinities up to 4.7 wt % eq NaCl [*Fouquet et al.*, 1991a, b]. The microthermometric results for

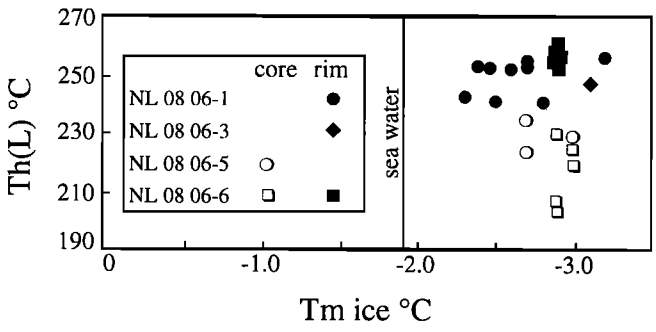


**Figure 14.** Correlation between Tm ice and Th(L) for fluid inclusions in sphalerites from the White Church field (sample NL 08 06). Several crystal portions (labeled NL 08 06-n) were used.

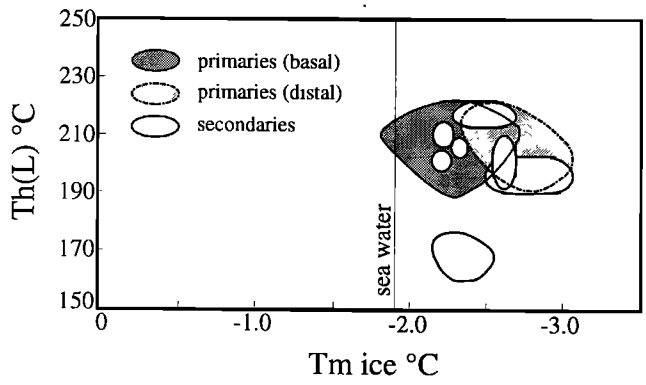


**Figure 15.** Correlation between Tm ice and Th(L) for fluid inclusions in coarse-grained barite from the Hine Hina field (sample NL 16 02). "Basal" and "distal" refer to fluid inclusions close to the basis and the top of the crystal, respectively.

the Whitechurch sphalerite match well those for Vai Lili sphalerite as reported by *Herzig et al.* [1993] (Te -21°C; 5% wt % eq NaCl; formation temperature ≤ 280°C; mixing with seawater).

**5.3.3. Mixing of seawater with an unusual Mg-rich end-member (Hine Hina barite).** Consideration of the Th(L)-Tm ice relationships for the fluid inclusions in the NL 16 02 barite sample (Figure 15) indicates that (1) most secondary inclusions span the variations of the primary inclusions and (2) there are several trends of salinity variation at more or less constant temperatures that are interpreted as dilution trends reflecting the more or less isothermal mixing of the L2 end-member with seawater. This mixing is also apparent in Figure 8 with calculated fluid compositions that display a trend from a fluid with 2.1 wt % NaCl + 2.1 wt % $MgCl_2$ toward a fluid of composition similar to seawater. This trend is interpreted as a mixing trend between a hydrothermal end-member L2 and seawater. Compared to seawater, L2 is not only more saline but Ca-depleted, Mg-enriched, and slightly Na-depleted.

The L2 fluid composition is rather uncommon. It is well known that usual hydrothermal end-members in the seafloor systems are Mg-depleted and Ca-enriched due to exchange with magmatic Fe-Mg and Ca-silicates at temperatures higher than ≈150°C [e.g., *Seyfried and Mottl*, 1982]. However, Mg-bearing fluids are not unknown in the subseafloor environment. From alteration studies in the Deep Sea Drilling Project (DSDP) Hole 504B, *Honnorez et al.* [1985] deduced the existence of fluids leaching the magnesium from basalts at low temperatures (<250°C) and that lead to Mg-bearing fluids which are able to precipitate Mg-silicates. Moreover, *McMurtry et al.* [1993] reported the existence of Mg-enriched hydrothermal fluids relatively to seawater that were venting at low temperature (≤40°C) on the Kasuga Sea Mount of the Mariana Arc. Compared with seawater, these fluids are also depleted in Ca (-64%) and have similar Na contents. They are interpreted as hydrothermal fluids derived from seawater, mixed with magmatic gases, and that resulted from a low-temperature (<150-200°C) "chemical weathering" of Mg-rich phases already present in altered basalts [*McMurtry et al.*, 1993]. These Mg-bearing fluids could be compared with the Hine Hina L2 end-member.

**5.3.4. Mixing of seawater with a condensed vapor.** Considering the Sr data for the coeval barite inclusions in sphalerite, the fluids in the barite sample (NL 22 06) may be interpreted as the result of a mixing process between seawater and a very low-salinity fluid, possibly close to pure water. Since the involvement of meteoric water is precluded in the Lau environment, this low-salinity fluid is likely a condensed vapor.

### 5.4. The Origin of High $\delta^{18}O$ Values

Using the model depicted in Figure 13, it is concluded that reasonable water-rock ratios (equal or higher than 0.1) require temperatures above 450°C for obtaining the high $\delta^{18}O$ values (5.2‰) of the hydrothermal end-member (L1) at the Vai Lili site. Even for unrealistically very low ratios, temperatures higher than 410°C should be required. In the same way, a minimal temperature of 320°C is required to explain the observed $\delta^{18}O$ values in the Hine Hina barite by water-rock interaction alone.

Only if high temperatures (>400°C) are considered in the HTRZ, the $^{18}O$ enrichment of the L1 fluids may have resulted from very low water-rock interactions alone. Such high temperatures are possible at Vai Lili, since temperatures as high a 400°C were measured on active black smokers [*Fouquet et al.*, 1991a]. However, considering that the Sr isotope composition of the present-day fluid at Vai Lili (0.7044 [*Fouquet et al.* 1991b]) indicates water-rock ratios in the HTRZ around 1.5 [*Fouquet et al.*, 1993], very low water-rock ratios at the origin of $^{18}O$ enrichment of L1 are considered unlikely. At Hine Hina the required temperature is too high for the source zone of the unusual L2 end-member (see above).

Classical "box-models" of water-rock interactions cannot explain entirely the high $\delta^{18}O$ values of the Lau basin fluids. On the other hand, chromatographic models of fluid-rock interaction could explain the observed $^{18}O$ enrichments. Nevertheless, we emphasize the absence of correlation between the strontium and oxygen isotope compositions (Table 1) that would be expected if oxygen isotope compositions in the end-members resulted from water-rock interactions. Therefore we must look for other processes such as phase separation and magmatic contribution. As phase separation alone is likely unable to produce the observed $\delta^{18}O$ values, a magmatic contribution must be conceived.

### 5.5. The Origin of High Salinities: Phase Separation From Seawater or From Magma?

As seen in Figure 12, at any temperature above 360°C at the depth of the HTRZ in the Vai Lili field (point C), the ascent of heated seawater along an adiabatic path would normally lead to phase separation, eventually yielding some saline liquids. This is a consequence of the shallow setting of the Lau basin hydrothermal fields. The fluid pressure at the HTRZ in the Vai Lili field is estimated at 270 bars, assuming that the pressure gradient is hydrostatic: a reasonable assumption in the brittle part of the oceanic crust [*Goldfarb and Delaney*, 1988]. However, the salinity of these final brines cannot be higher than ≈15 wt % NaCl (Figure 12, point A) and, moreover, the volumes of produced brines are likely to be very small. Nevertheless, the phase separation process may contribute to explain the salinities systematically higher than those of seawater observed in the Lau basin venting fluids [*Fouquet et al.*, 1991a, b] and in sphalerite fluid inclusions at Vai Lili [*Herzig et al.* , 1993; this study]. The low-salinity fluids trapped into the Vai Lili NL 22 06 barite may be representative of the vapors generated by the same process.

To produce the high-salinity liquid (30 wt % eq NaCl) measured in the fluid inclusions of the Vai Lili BL 12 anhydrite, we may consider phase separation either from seawater or from a magma. Considering phase separation from heated seawater in the Vai Lili system, it may be concluded that two of the three processes discussed in section 5.2.1 may have been operative to yield a high-salinity brine. Adiabatic phase separation is plausible but requires very hot fluids: intersection of the $(L+V)_{30}$ curve (at very shallow depth: point D in Figure 12) can be achieved only by seawater initially hotter than 485°C and intersecting the $(L+V)_{sw}$ curve at ≈500 bars (Figure 12, point E). This would approximately correspond to the depth of the imaged magmatic chamber under the Vai Lili field at 2 km below the estimated HTRZ [*Morton and Sleep*, 1985; *Collier and Sinha*, 1990]. In that case, the phase separation process would deeply affect infiltrated seawater approaching the magma chamber. Isobaric heating is also conceivable, as discussed in section 5.2.1.2. Isothermal decompression is unlikely because the shallow depth of the permanent magmatic chamber seems to preclude the existence of the required elevated thermal gradient.

Although phase separation from seawater is able to yield brines of the required salinity under the Vai Lili vents, it remains difficult to explain in that case how the vapors and brines are segregated, since they do not appear together in the vents. Moreover, when moving along open upflow conduits, the separated phases form a well-mixed two-phase fluid [*Goldfarb and Delaney*, 1988]. Venting fluids are likely to be ultimately remixed fluids that are less saline than the initially separated brine as observed in the TAG hydrothermal system [*Petersen et al.*, 1998].

On the other hand, phase separation from the hydrous fluid exsolved from a magma yields a small volume of brine that could possibly explain the paucity of brines at the seafloor level. Three kilometers below seafloor, phase separation would occur in narrow cracks and would favor the segregation of vapor and liquid. The liquid would remain at depth while the vapor would be evacuated toward the seafloor [*Goldfarb and Delaney*, 1988]. The reality of such a segregation process has been recently documented in some active chimneys of the East Pacific Rise [*von Damm et al.*, 1997]. Accidental release of the segregated brine could be favored by the tectonic setting of the Vai Lili hydrothermal system that is mainly controlled by a major normal fault [*Fouquet et al.*, 1993].

## 6. Conclusion

The results of this study emphasize the specificity of oceanic hydrothermal systems in back arc settings well illustrated by the Lau basin. In addition to the well-known influence of this non-mid-ocean ridge setting on the chemistry of venting fluids [*Fouquet et al*, 1993; and references therein], the shallow level of the hydrothermal systems favors phase separation processes compared to the deep-seated MOR hydrothermal systems. The importance of silicic magmatism at the ridge provides a source of both heat and water-rich saline fluids in the upper levels of the hydrothermal systems. In the Lau basin, phase separation and magmatic fluids both contribute to the existence of saline hydrothermal end-members (≥ 5.5 wt % eq NaCl) with high

$\delta^{18}O$ values (≥5‰). The back arc setting also explains the presence of unusual fluids such as the 30 wt % NaCl brine found in anhydrite or the Mg-rich end-member observed in barite. The oxygen isotope compositions of hydrothermal fluids venting in the Lau basin reveal that seawater is $^{18}O$-enriched during on-axis hydrothermal activity in back arc basins.

**Acknowledgments.** This work was supported by the PNEHO program. J. Pironon (CREGU, Nancy, France) kindly provided the micro-Raman determinations in fluid inclusions. Two anonymous reviewers, D.S. Stakes, and A.E. Kohn are warmly acknowledged for their stimulating criticism of the first drafts of this paper.

## References

Albarède, F., A. Michard, J.F. Minster, and G. Michard, $^{87}Sr/^{86}Sr$ ratios in hydrothermal waters and deposits from the East Pacific Rise at 21°N, *Earth Planet. Sci. Lett.*, *55*, 229-236, 1981.

Baumgartner, L.P., and D. Rumble, Transport of stable isotopes, I, Development of a kinetic continuum theory for stable isotope transport, *Contrib. Mineral. Petrol.*, *98*, 417-430, 1988.

Bischoff, J.L., Geothermal systems at 21°N, East Pacific Rise: Physical limits of geothermal fluids and role of adiabatic expansion, *Science*, *207*, 1465-1469, 1980.

Bischoff, J.L., and K.S. Pitzer, Phase relations and adiabats in boiling seafloor geothermal systems, *Earth Planet. Sci. Lett.*, *75*, 327-338, 1985.

Bischoff, J.L., and K.S. Pitzer, Liquid-vapor relations for the system NaCl-$H_2O$: Summary of the P-T-x surface from 300 to 500°C, *Am.J. Sci.*, *289*, 217-248, 1989.

Bischoff, J.L., and R.J. Rosenbauer, The critical point and two-phase boundary of seawater, 200-500°C, *Earth Planet. Sci. Lett.*, *68*, 172-180, 1984.

Bischoff, J.L., and R.J. Rosenbauer, An empirical equation of state for hydrothermal sawater (3.2 percent NaCl), *Am.J. Sci.*, *285*, 725-763, 1985.

Bodnar, R.J., Revised equation and table for determining the freezing point depression of $H_2O$-NaCl solution, *Geochim. Cosmochim. Acta*, *57*, 683-684, 1993.

Bodnar, R.J., Synthetic fluid inclusions, XI, The system $H_2O$-NaCl: Experimental determination of the halite liquidus and isochores for a 40 wt% NaCl solution, *Geochim. Cosmochim. Acta*, *58*, 1053-1063, 1994.

Bodnar, R.J., C.W. Burnham, and S.M. Sterner, Synthetic fluid inclusions in natural quartz, III, Determination of phase equilibrium properties in the system $H_2O$-NaCl to 1000°C and 1500 bars, *Geochim. Cosmochim. Acta*, *49*, 1861-1873, 1985.

Boespflug, X., L. Dosso, H. Bougault, and J.L. Joron, Trace element and isotopic (Sr, Nd) geochemistry of volcanic rocks from the Lau Basin, *Geol. Jahrb.*, *92*, 503-516, 1990.

Butterfield, D.A., G.J. Massoth, R.E. McDuff, J.E. Lupton, and M.D. Lilley, Geochemistry of hydrothermal fluids from axial seamount hydrothermal emissions study vent field, Juan de Fuca Ridge: Subseafloor boiling and subsequent fluid-rock interaction, *J. Geophys. Res.*, *95*, 12895-12921, 1990.

Cathles, L.M., A.L. Guber, T.C. Lenagh, and F.O. Dudas, Kuroko-type massive sulfide of Japan: Product of an aborted island-arc rift, in *Econ. Geol. Monogr.*, *5*, 96-114, 1983.

Chiba, H., and H. Sakai, Oxygen isotope exchange between dissolved sulfate and water at hydrothermal temperatures, *Geochim. Cosmichim. Acta*, *49*, 993–1000, 1985.

Cline, J.S., and R. Bodnar, Can economic copper mineralization be generated by a typical calc-alkaline melt?, *J. Geophys. Res.*, *96*, 8113-8126, 1991.

Cocker, J.D., B.J. Griffin, and K. Muehlenbachs, Oxygen and carbon isotope evidence for seawater-hydrothermal alteration of the Macquarie Island ophiolite, *Earth Planet. Sci. Lett.*, *61*, 112-122, 1982.

Collier, J., and M. Sinha, Seismic images of a magma chamber beneath the Lau Basin back-arc spreading centre, *Nature*, *346*, 646-648, 1990.

Crawford, M.L., Phase equilibria in aqueous fluid inclusions, in *Short Course in Fluid Inclusions: Applications to Petrology*, edited by L.S. Hollister and M.L. Crawford, pp. 75-100, Mineral. Assoc. of Can., 1981.

Delaney, J.R., D.W. Mogk, and M.J. Mottl, Quartz-cemented breccias from the Mid-Atlantic Ridge: Samples of a high-salinity hydrothermal upflow zone, *J. Geophys. Res.*, *92*, 9175-9192, 1987.

Dhamelincourt, P., J. Beny, J. Dubessy, and B. Poty, Analyse d'inclusions fluides à la microsonde MOLE à effet Raman, *Bull. Mineral.*, *102*, 600-610, 1979.

Dubois, M., and C. Marignac, The $H_2O$-NaCl-$MgCl_2$ ternary phase diagram with special application to fluid inclusion studies, *Econ. Geol.*, *92*, 114-119, 1997.

Foucher, J.P., and Shipboard Scientific Party, La ride de Valu Fa dans le bassin de Lau méridional (sud-ouest Pacifique), *C. R. Acad. Sci. Paris*, *307*,(II), 609-616, 1988

Fouillac, A.M., and M. Javoy, Oxygen and hydrogen isotopes in the volcano-sedimentary complex of Huelva (Iberian Pyrite Belt): Example of water circulation through a volcano-sedimentary sequence, *Earth Planet. Sci. Lett*, *87*, 473-484, 1988.

Fouquet, Y., and E. Marcoux, Lead isotope systematics in Pacific hydrothermal sulfide deposits, *J. Geophys. Res.*, *100*, 6025-6040, 1995.

Fouquet, Y., et al., Hydrothermal activity and metallogenesis in the Lau back-arc basin, *Nature*, *349*, 778-781, 1991a.

Fouquet, Y., et al., Hydrothermal activity in the Lau back-arc basin: Sulfides and water chemistry, *Geology*, *19*, 303-306, 1991b.

Fouquet, Y., U. von Stackelberg, J.L. Charlou, J. Erzinger, P.M. Herzig, R. Muhe, and M. Wiedicke, Metallogenesis in back-arc environments: The Lau basin example, *Econ. Geol.*, *88*, 2154-2181, 1993.

Franklin, J.M., J.W. Lydon, and D.F. Sangster, Volcanic associated massive sulfide deposits, *Econ. Geol. 75th Anniv. Vol.*, 485-627, 1981.

Frenzel, J.M., R. Mühe, and P. Stoffers, Petrology of the volcanic rocks from the Lau basin, Southwest Pacific, *Geol. Jahrb.*, *92*, 395-479, 1990.

Fujino, K., E.L. Lewis, and R.G. Perkins, The freezing point depression of seawater at pressures up to 100 bars, *J. Geophys. Res.*, *79*, 1792-1797, 1974.

Goldfarb, M.S., and J.R. Delaney, Response of two-phase fluids to fracture configurations within submarine hydrothermal systems, *J. Geophys. Res.*, *93*, 4585-4594, 1988.

Halbach, P., et al., Probable modern analogue of Kuroko-type massive sulphide deposits in the Okinawa Trough back-arc basin, *Nature*, *338*, 496-499, 1989.

Hawkins, J.W., and J.T. Melchior, Petrology of Mariana trough and Lau basin basalts, *J. Geophys Res.*, *90*, 11431-11468, 1985.

Haynes, F.M., Determination of fluid inclusion composition by sequential freezing, *Econ. Geol.*, *80*, 1436-1439, 1985.

Hedenquist, J.W., Adiabatic boiling and ocean metal transport, *Nature*, *310*, 636, 1984.

Herzig, P., U. von Stackelberg, and S. Petersen, Hydrothermal mineralization from the Valu Fa Ridge, Lau back-arc basin (SW Pacific), *Mar. Min.*, *9*, 271-301, 1990.

Herzig, P.M., M.D. Hannington, Y. Fouquet, U. von Stackelberg, and S. Petersen, Gold in seafloor polymetallic sulfides from the Lau back-arc and implication for the geochemistry of gold in volcanogenic massive sulfide deposits, *Econ. Geol.*, *88*, 2182-2209, 1993.

Honnorez, J., J.C. Alt, B.-M. Honnorez-Guerstein, C. Laverne, K. Muehlenbachs, J. Ruiz, and E. Saltzman, Stockwork-like sulfide mineralization in young oceanic crust: Deep sea drilling project hole 504B, *Initial Rep. Deep Sea Drill. Proj.*, *LXXXIII*, 263-282, 1985.

Horita, J., D.R. Cole, and D.J. Wesolowski, The activity-composition relationship of oxygen and hydrogen isotopes in aqueous salt solutions, III, Vapor-liquid water equilibration of NaCl solutions to 350°C, *Geochim. Cosmochim. Acta*, *59*, 1139-1151, 1995.

Jenner, G.A., P.A. Cawood, M. Rautenschlein, and W.M. White, Composition of back-arc volcanics, Valu Fa Ridge, Lau Basin: Evidence for a slab-derived component in their mantle source, *J. Volcanol. Geotherm. Res.*, *32*, 209-222, 1987.

Kishima, N., and H. Sakai, Oxygen-18 and deuterium determination on a single water sample of a few milligrams, *Anal. Chem.*, *52*, 356-358, 1980.

Lassey, K.R., and P. Blattner, Kinetically controlled oxygen isotope exchange between fluid and rock in one-dimensional advective flow, *Geochim. Cosmochim. Acta*, *52*, 2169-2175, 1988.

Lécuyer, C., and S. Fourcade, Oxygen isotope evidence for multi-stage hydrothermal alteration at a fossil slow-spreading center: The

Silurian Trinity ophiolite (California, U.S.A.), *Chem. Geol.*, *87*, 231-246, 1991.

Loock, G., W.F. Mc Donough, S L. Goldstein, and A.W. Hofmann, Isotopic composition of volcanic glasses from the Lau Basin, *Mar. Min.*, *9*, 235-245, 1990.

Lowell, R.P., P.A. Rona, and R.P. von Herzen, Seafloor hydrothermal systems, *J. Geophys. Res.*, *100*, 327-352, 1995.

McMurtry, G.M., P.N. Sedwick, P. Fryer, D.L. Von der Haar, and H.-W. Yeh, Unusual geochemistry of hydrothermal vents on submarine arc volcanoes: Kasuga Seamounts, northern Mariana Arc, *Earth Planet. Sci. Lett.*, *114*, 517-528, 1993.

Morton, J.. and W. Pohl, Magnetic anomaly identification in the Lau Basin and North Fiji basin, Southwest Pacific Ocean, *Geol. Jahrb.*, *92*, 93-108, 1990.

Morton, J., and N.H. Sleep, Seismic reflections from a Lau Basin magma chamber, in *Geology and Offshore Resources of Pacific Island Arcs: Tonga Region*, Earth Sci. Ser., vol. 2, edited by D. Scholl and T. Vallier, pp. 441-453, 1985.

Nehlig, P., Interactions between magma chambers and hydrothermal systems: Oceanic and ophiolitic constraints, *J. Geophys. Res.*, *98*, 19621 19633, 1993.

O'Neil, J.R., and L.H. Adami, The oxygen isotope partition function ratio of water and the structure of liquid water, *J. Phys. Chem.*, *73*, 1553-1558, 1969.

O'Neil, J.R., and H.P.J. Taylor, The oxygen isotope and cation exchange chemistry of feldspars, *Am. Mineral.*, *52*, 1414-1437, 1967.

Parson, L.M., J.A. Pearce, B.J. Murton, and R.A. Hodkinson, Role of ridge jumps and ridge propagation in the tectonic evolution of the Lau back-arc basin, Southwest Pacific, *Geology*, *18*, 470-473, 1990.

Petersen, S., P.M. Herzig, and M.D. Hannington, Fluid inclusion studies as a guide to the temperature regime within the TAG hydrothermal mound, 26°N, Mid-Atlantic Ridge, *Proc. Ocean Drill. Program Sci. Results*, *158*, 163-176, 1988.

Poty, B., J. Leroy, and L. Jachimowicz, Un nouvel appareil pour la mesure des températures sous le microscope, l'installation de microthermométrie Chaix-Meca, *Bull. Soc. Fr. Mineral. Cristallogr.*, *99*, 182-186, 1976.

Roedder, E., Fluid inclusions, in *Reviews in Mineralogy*, vol. 12, Mineral. Soc. of Am., 644 pp., Washington, D.C., 1984.

Rona, P.A., Hydrothermal mineralization at oceanic ridges, *Can. Mineral.*, *26*, 431-465, 1988.

Sawkins, F.J., *Metal Deposits in Relation to Plate Tectonics, Minerals and Rocks*, vol. 17, 461pp., Springer-Verlag, New York, 1990.

Schiffman, P., A.E. Williams, and R.C. Evarts, Oxygen isotope evidence for submarine hydrothermal alteration of the Del Puerto ophiolite, California, *Earth Planet. Sci. Lett.*, *70*, 207-220, 1984.

Scott, S.D., Sea-floor polymetallic sulfide deposits: Modern and ancient, *Mar. Min.*, *5*, 191-212, 1985.

Scott, S.D., Sea-floor polymetallic sulfides: Scientific curiosities or mines of the future?, in *Marine Minerals: Advances in Research and Resources Assessment*, edited by P.G. Teleki, M.R. Dobson, J.R. Moore, and U. von Stackelberg, *NATO ASI Ser. C*, *194*, 277-300, 1987.

Seyfried, W.E., Jr., and M.J. Mottl, Hydrothermal alteration of basalt by seawater under sawater-dominated conditions, *Geochim. Cosmochim. Acta*, *46*, 985-1002, 1982.

Sheppard, S.M.F., Characterization and isotopic variations in natural waters, in *Stable Isotopes in High Temperature Geological Processes*, edited by J.W. Valley, H.P. Taylor, and J.R. O'Neil, pp. 165-183, Mineral. Soc. of Am., Washington, D.C., 1986.

Sterner, S.M., D.L. Hall, and R.J. Bodnar, Synthetic fluid inclusions, V, Solubility relations in the NaCl-KCl-$H_2O$ system under vapor-saturated conditions, *Geochim. Cosmochim. Acta*, *52*, 989-1005, 1988.

Sunkel, G., Origin of petrological and geochemical variations of Lau basin lavas (SW Pacific), *Mar. Min.*, *9*, 205-234, 1990.

Taylor, H.P.J., Water/rock interactions and the origin of $H_2O$ in granitic batholiths, *J. Geol. Soc. London*, *133*, 509-558, 1977.

Tivey, M.K., R.A. Mills, and D.A.H. Teagle, Temperature and salinity of fluid inclusions in anhydrite as indicators of seawater entrainment and heating in the TAG active mound, *Proc. Ocean Drill. Program Sci. Results*, *158*, 179-190, 1998.

Vanko, D.A., R.J. Bodnar, and S.M. Sterner, Synthetic fluid inclusions, VIII, Vapor-saturated halite solubility in part of the system NaCl-$CaCl_2$-$H_2O$, with application to fluid inclusions from oceanic hydrothermal systems, *Geochim. Cosmochim. Acta*, *52*, 2451-2456, 1988.

Volpe, A. M., J.D. Macdougall, and J.W. Hawkins, Lau basin basalts (LBB): Trace element and Sr-Nd isotope evidence for heterogeneity in back-arc basin mantle, *Earth Planet. Sci. Lett.*, *90*, 174-176, 1988.

von Damm, K.L , L.G. Buttermore, S E. Oosting, A.M. Bray, D.J. Fornari, M.D. Lilley, and W.C. Shanks, III, Direct observation of the evolution of a seafloor "black smoker" from vapor to brine, *Earth Planet. Sci. Lett.*, *149*, 101-111, 1997.

von Stackelberg, U., and Shipboard Scientific Party, Active hydrothermalism in the Lau back-arc basin (SW-Pacific): First results from the SONNE 48 cruise (1987), *Mar. Min.*, *7*, 431-442, 1988.

von Stackelberg, U., and U. von Rad, Geological evolution and hydrothermal activity in the Lau and North Fiji Basins (SONNE cruise SO-35)- A synthesis, *Geol. Jahrb.*, *92*, 629-660, 1990.

Zhang, Y.G., and J.D. Frantz, Determination of the homogenization temperatures and densities of supercritical fluids in the system NaCl-KCl-$CaCl_2$-$H_2O$ using synthetic fluid inclusions, *Chem. Geol.*, *64*, 335-350, 1987.

Michel Dubois, Sciences de la Terre, Université des Sciences et Technologies de Lille, 59655 Villeneuve d'Ascq, France.

Yves Fouquet, IFREMER, Centre de Brest, BP70, 29280 Plouzane, France.

Gérard Gruau, Géosciences Rennes, CNRS UPR 4661, Université de Rennes I, Campus de Beaulieu, Avenue du Général Leclerc, 35042 Rennes, France

Christophe Lécuyer, Laboratoire de Sciences de la Terre, CNRS UMR 5570, Ecole Normale Supérieure de Lyon, 46, Allée d'Italie, 69364 Lyon, cedex 07, France. (e-mail: clecuyer@geologie.ens-lyon.fr)

Christian Marignac, Ecole des Mines de Nancy, 54042 Nancy and CRPG-CNRS, BP 20, 54501 Vandoeuvre-lès-Nancy, France

Claire Ramboz, CRSCM-CNRS, 1A rue de la Férollerie, 45071 Orléans, France

(Received February 26, 1998; revised February 15, 1999;
accepted March 19, 1999)